

Pedo-geochemistry of Vertisols Under Tropical Seasonally Contrasted Climate, Northern Cameroon: Implications for Vertisolization

Gouban Hamadjida^{1,2}, Lionelle Estelle Bitom-Mamdem¹, Jean Pierre Temga^{1,*}, Elisé Sababa¹, Primus Tamfuh Azinwi³, Simon Djakba Basga⁴, Elisabeth Yaboki⁴, Jean Pierre Nguetnkam⁵, Dieudonné Lucien Bitom^{1,3}

¹Department of Earth Sciences, Faculty of Science, University of Yaounde I, Yaounde, Cameroon

²National Institute of Cartography, Yaounde, Cameroon

³Department of Soil Science, Faculty of Agronomy and Agricultural Sciences, Dschang, Cameroon

⁴Institute of Agricultural Research for Development, Garoua, Cameroon

⁵Department of Earth Sciences, Faculty of Science, University of Ngaoundere, Ngaoundere, Cameroon

Email address:

temgajp@yahoo.fr (J. P. Temga)

*Corresponding author

To cite this article:

Gouban Hamadjida, Lionelle Estelle Bitom-Mamdem, Jean Pierre Temga, Elisé Sababa, Primus Tamfuh Azinwi, Simon Djakba Basga, Elisabeth Yaboki, Jean Pierre Nguetnkam, Dieudonné Lucien Bitom. Pedo-geochemistry of Vertisols Under Tropical Seasonally Contrasted Climate, Northern Cameroon: Implications for Vertisolization. *Earth Sciences*. Vol. 11, No. 4, 2022, pp. 171-193.
doi: 10.11648/j.earth.20221104.14

Received: June 7, 2022; **Accepted:** June 29, 2022; **Published:** July 22, 2022

Abstract: Fourthly one representative profile of Northern Cameroon Vertisols on lowland and upland areas under tropical seasonally contrasted climate were investigated to assess the genesis of smectite and vertisolization processes on their geochemistry relation. Macro-micromorphological, physico-chemical, mineralogical and geochemical properties were determined for 137 soil samples. Statistical analysis was used to interpret the dataset and identify affinity groups of samples and properties. Dark gray color, slickensides, cracks and micro relief gilgai are major characteristics of the soils within the abundance of the major mineral constituents: smectite, kaolinite and quartz. Silicon, Al and Fe were the most abundant elements in Vertisols. Vertisols developed upland and lowland under tropical seasonally contrasted climate showed the following orders for REE concentrations: Ce > Nd > La > Pr > Sm > Gd > Dy > Yb > Er > Eu > Ho > Tb > Lu > Tm and Ce > La > Nd > Pr > Sm > Gd > Dy > Yb > Er > Eu > Ho > Tb > Lu > Tm, respectively. The grouping of properties into affinity groups is mostly weak with properties showing a diffuse distribution with no very distinct affinity groups. In the upland Vertisols, genesis of the smectites is made from the feldspars present in the parent rock; meanwhile, high smectite content was related to the low landscape positions, a strongly contrasted climate and the presence of a clay-rich alluvial parent material in lowland Vertisols. Climates with contrasting seasons, there is intense weathering during the wet season. The released ions are concentrated in the dry season and give smectite. This concentration can take place on site on basic or acid crystal rocks, or in the low points of the landscape.

Keywords: Cameroon, Tropical Contrasting Seasons, Vertisols, Pedological, Geochemistry, Vertisolization Process

1. Introduction

Vertisols occupy about 311 million ha of land, that is, about 2.42% of ice-free land, out of which 150 million ha is potential cropland [16]. It occurs mainly in the intertropical zone covering about 200 million hectares (4% of land surface).

Vertisols form a considerable agricultural potential but adapted management is a precondition for sustained production [52]. Vertisols are chemically very fertile in the natural state and this particularity makes them very attractive for agricultural purposes [17, 33]. Although, their physical properties make the very difficult of agricultural exploitation

[21]. This explains why their agriculture potentials have not yet been fully exploited in many parts of the world, especially in the Sub-saharan zone where widespread areas of Vertisols are either left fallow or used for grazing and woodland for charcoal burning [18]. However, lowland Vertisols are used for paddy rice cultivation and upland Vertisols are used for field crops [9].

Vertisols are tropical soils that form under contrasted climate with a well-marked dry season alternating with a wet one [45]. They are characterized by at least 30% clay fraction, abundance of smectitic swelling clay minerals, a high cation exchange capacity (20 – 45 meq/100g of soil) and a high base saturation (80 – 100%) [59]. The swelling and shrinking upon wetting and drying is the major characteristic of these soils [21, 29]. Based on their smectite content, these soils present numerous interesting economic potentials in the chemical industry, pharmaceuticals, agronomy and environmental protection [44, 59]. So, pedological processes play a more important role in determining the chemical composition of these soils than does depositional layering.

Accordingly, in this paper we present and discuss pedological and geochemical results concerning the analysis of the upland and lowland Vertisols samples under tropical seasonally contrasted climate in Northern Cameroon.

Geochemistry of Vertisols in this zone has not been previously investigated, particularly regarding the genesis of smectite and vertisolization processes.

2. Geological Setting

The study area concerns Northern Cameroon and extends from 8°00' to 13°30'N and 12°00' to 16°00'E (Figure 1). Its area is estimated at 82,500 km². The distribution of precipitation subjects the whole zone to a tropical climate with two very contrasting seasons. Average annual rainfall ranges from 500 mm to 1,500 mm. The rainy season lasting 7 months to the South of Benue (from April to October) is reduced to 3 months (June to August) in the Chari region. The average annual temperature varies from 30 to 35°C with monthly minima of 12 to 15°C in December and January. The relative humidity is 80% in the rainy season and it drops to 30 or 40%, sometimes to less than 10%, in the dry season. Two geological formations occupy most of the area: the granito-gneissic basement and the alluvium of the Chad basin. In addition, we observe various formations, scattered in the basement; those are sedimentary basins, metamorphic series, basic rocks and recent alluvium, covering an area less than 20% (Figure 1).

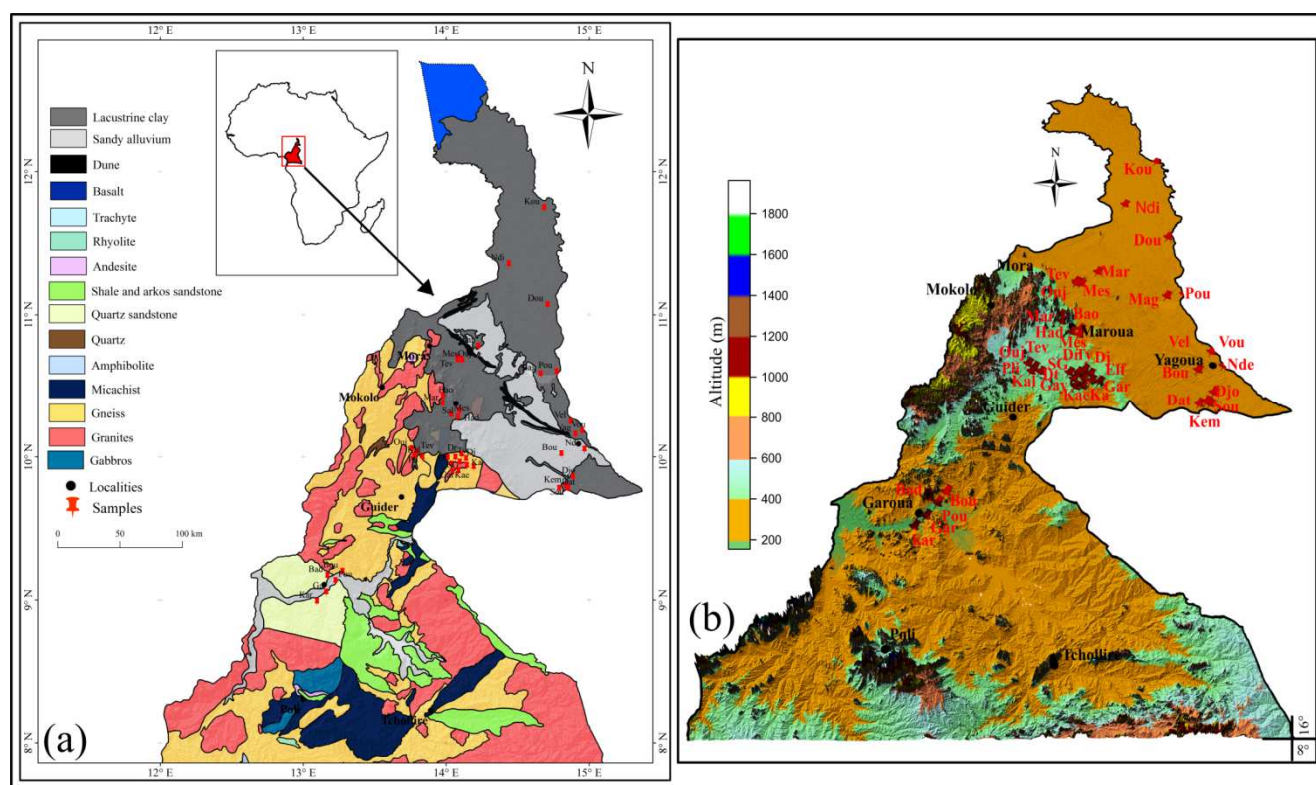


Figure 1. Study area: (a) geological setting, (b) Block diagram showing the main geomorphological units and soil sampling sites for Northern Cameroon Vertisols.

In Cameroon, Vertisols are essentially signaled in the sudano-sahelian zone of Northern Cameroon [6]. They occupy a total surface area of 25,000 km², specifically in the Benue watershed and the Chad basin [59]. Two main types of Vertisols can be distinguished: upland Vertisols and lowland

Vertisols [3]. The upland Vertisols are developed on various parent rocks whose weathering generates base-rich environments favorable for smectite synthesis, while lowland Vertisols formation is favored by low landscape positions favorable for accumulation of basic cations [15].

Lowland Vertisols are more widespread and occur mainly in the Diamare, Kaele, Logone and Chari plains, and the Benue through [45]. Upland Vertisols are more localized; they form on calco-alkaline granites, gneiss and other ferromagnesian rocks in North Cameroon [63]. Regarding the topographic position, lowland Vertisols are always observed in the low position, with reduced external drainage or on variant slopes between 1 and 2%, while the upland Vertisols can occupy higher positions.

3. Materials and Methods

3.1. Area Characterization

The study was carried out on Cameroon Vertisols developed under a tropical seasonally contrasted climate. Vertisols are widely distributed in the Northern Cameroon. They have developed on alluvium, granite, gneiss and metadiorite (Figure 1, Table 1). The environmental setting, land use and

classification following Soil Taxonomy were recorded [56]. Lowland Vertisols are observed in lower areas with an altitude below 300m while upland Vertisols occupy slightly high with an altitude of 300 to 500m.

3.2. Soil Sampling

The study was carried out on twenty-two lowland Vertisols and nineteen upland Vertisols. Soil profiles were dug at the end of the rainy season (mid-November) to avoid rainy season inundations that make Vertisols very sticky and excessive dry season that render the Vertisols too hard to break. Soils descriptions and soil classification was based on the USDA Soil Taxonomy [56]. Soil color was determined on moist soils by reference to Munsell soil color charts [37] (Table 1). Lowland Vertisols, with A(BgC or A(B)Cg profile and upland ones, characterized by A(B)C profile type. On each profile, samples were collected at different depths. A total of 137 soil samples have been collected and analysed.

Table 1. Classification and environmental of Northern Cameroon Vertisols.

Site (Samples)	Classification	Landform	Parent material	Location	
Lowland Vertisols					
Garoua (Gar)	Typic Endoaquerts	Lower flood plain	Alluvium	9°15' N	13°24' E
Pouimpoumre (Pou)	Chromic Endoaquerts	Sub-horizontal flat plain	Alluvium	9°20' N	13°28' E
Bounguel (Bou)	Chromic Endoaquerts	Alluvial plain	Alluvium	9°24' N	13°31' E
Badoudi (Bad)	Typic Endoaquerts	Sub-horizontal flat plain	Alluvium	10°13' N	13°34' E
Karewa (Kar)	Aridic Endoaquerts	Sub-horizontal flat plain	Alluvium	9°11' N	13°20' E
Forfourou (For)	Aridic Endoaquerts	Local alluvial plain	Alluvium		
Koussérie (Kou)	Chromic Endoaquerts	Sub-horizontal flat plain	Alluvium	12°05' N	14°25' E
Doublé (Dou)	Typic Endoaquerts	Sub-horizontal flat plain	Alluvium	11°20' N	15°00' E
Ndiguina (Ndi)	Chromic Endoaquerts	Alluvial plain	Alluvium	11°49' N	14°27' E
Makari (Mak)	Aridic Endoaquerts	Flat plain	Alluvium	11°50' N	14°06' E
Vounaloum (Vou)	Chromic Endoaquerts	Alluvial plain	Alluvium	10°25' N	15°15' E
Velé (Vel)	Typic Endoaquerts	Lower flood plain	Alluvium	10°29' N	15°10' E
Ndehé (Nde)	Chromic Endoaquerts	Alluvial plain	Alluvium	10°17' N	15°16' E
Bougaye (Bou)	Aridic Endoaquerts	Local alluvial plain	Alluvium	10°15' N	15°06' E
Yagoua (Yag)	Chromic Endoaquerts	Alluvial plain	Alluvium	10°30' N	15°35' E
Djondong (Djo)	Typic Endoaquerts	Lower flood plain	Alluvium	10°05' N	15°11' E
Soukoumkaya (Sou)	Chromic Endoaquerts	Alluvial plain	Alluvium	10°00' N	15°09' E
Datchéka (Dat)	Typic Endoaquerts	Lower flood plain	Alluvium	10°00' N	15°05' E
Kembe (Kem)	Chromic Endoaquerts	Alluvial plain	Alluvium	10°01' N	15°08' E
Pouss (Pou)	Typic Endoaquerts	Lower flood plain	Alluvium	10°51' N	15°04' E
Maga (Mag)	Chromic Endoaquerts	Alluvial plain	Alluvium	10°50' N	14°57' E
Manga (Man)	Aritic Endoaquerts	Local alluvial plain	Alluvium		
Upland Vertisols					
Kaélé 1 (Kae)	Chromic Haplusterts	Lower footslope	Granite	10°06'55"	14°27'11"E
Kaélé 2 (Ka)	Typic Haplusterts	Upper footslope	Granite	10°06'39"N	14°25'41"E
Garey 1 (Gar)	Typic Haplusterts		Granite	10°02'02"N	14°20'27"E
Garey 2 (SG)	Calcic Haplusterts		Granite	10°01'52"N	14°19'36"E
Garey 3 (Gay)	Calcic Haplusterts		Granite	10°05' N	658E
Djidoma (Dj)	Chromic Haplusterts	Lower footslope	Granite	10°05' N	143E
Tipili Yewey (TY)	Typic Haplusterts		Granite	10°05' N	605E
Elf (ELF)	Chromic Haplusterts	Lower footslope	Granite	10°06' N	550E
Dardo Tipili (DT)	Calcic Haplusterts		Granite	10°05' N	637E
Drame (DR)	Typic Haplusterts		Granite	10°05' N	637E
Maroua (Mar)	Calcic Haplusterts		Métadolerite	10°62' N	14°30' E
Baoliol (Bao)	Calcic Haplusterts		Métadolerite	10°64' N	14°27' E
Hadango (Had)	Typic Haplusterts		Métadolerite	10°67' N	14°27' E
Salak (Sal)	Chromic Haplusterts	Lower footslope	Métadolerite	10°45' N	
Plim (Pli)	Chromic Haplusterts	Lower footslope	Gneiss		
Tevan (Tev)	Typic Haplusterts	Upper footslope	Gneiss	10°57' N	14°21' E
Ouji (Ouj)	Calcic Haplusterts	Upper footslope	Gneiss	10°56' N	14°21' E
Meskine (Mes)	Typic Haplusterts	Upper footslope	Gneiss	10°56' N	14°23' E

Table 1. Continued.

Site (Samples)	Elevation (m)	Land use	Data source
Lowland Vertisols			
Garoua (Gar)	175	Dry-season sorghum	Azinwi Tamfuh et al., 2016
Pouimpoumre (Pou)	180	Dry-season sorghum	Azinwi Tamfuh et al., 2016
Bounguel (Bou)	178	Dry-season sorghum	Azinwi Tamfuh et al., 2016
Badoudi (Bad)	173.6	Rainy sorghum	Azinwi Tamfuh et al., 2016
Karewa (Kar)	191	Dry-season sorghum	Azinwi Tamfuh et al., 2016
Forftourou (For)		Dry-season sorghum	Nguetnkam, 2004
Koussérie (Kou)	260	Dry-season sorghum	Nguetnkam, 2004
Doublé (Dou)	320	Dry-season sorghum	Temga et al., 2019
Ndiguina (Ndi)	299	Dry-season sorghum	Temga et al., 2019
Makari (Mak)	250	Dry-season sorghum	Ekodeck, 1976
Vounaloum (Vou)	328	Irrigated paddy	Basga et al., 2018
Velé (Vel)	314	Irrigated paddy	Basga et al., 2018
Ndehé (Nde)	330	Rainfed paddy	Basga et al., 2018
Bougaye (Bou)	334	Dry-season sorghum	Basga et al. 2018
Yagoua (Yag)	330	Rainy sorghum	This study
Djondong (Djo)	325	Rainy sorghum	This study
Soukoumkaya (Sou)	334	Rainy sorghum	This study
Datchéka (Dat)	336	Rainy sorghum	This study
Kembe (Kem)	330	Irrigated paddy	This study
Pouss (Pou)	320	Irrigated paddy	This study
Maga (Mag)	321	Irrigated paddy	This study
Manga (Man)	334	Rainy sorghum	This study
Upland Vertisols			
Kaélé 1 (Kae)	367	Rainy sorghum	Nguetnkam, 2004
Kaélé 2 (Ka)	381	Rainy sorghum	Nguetnkam et al., 2007
Garey 1 (Gar)	373	Dry-season sorghum	Nguetnkam et al., 2007
Garey 2 (SG)	378	Dry-season sorghum	Nguetnkam et al., 2007
Garey 3 (Gay)	368	Dry-season sorghum	This study
Djidoma (Dj)	380	Rainy sorghum	This study
Tipili Yewey (TY)	376	Dry-season sorghum	This study
Elf (ELF)	375	Dry-season sorghum	This study
Dardo Tipili (DT)	382	Rainy sorghum	This study
Drame (DR)	377	Rainy sorghum	This study
Maroua (Mar)	427	Rainy sorghum	This study
Baoliol (Bao)	423	Dry-season sorghum	This study
Hadango (Had)	440	Dry-season sorghum	This study
Salak (Sal)	424	Dry-season sorghum	This study
Plim (Pli)	412	Dry-season sorghum	This study
Tevan (Tev)	416	Dry-season sorghum	This study
Ouji (Ouj)	445	Dry-season sorghum	This study
Meskine (Mes)	428	Dry-season sorghum	This study

3.3. Analytical Methods

3.2.1. Micromorphological Observation

Micromorphological observations were made according to Fitz [22], while interpretation of micromorphological features followed the criteria of Stoops et al. [57]. According to these methods, undisturbed soil samples were first air-dried, impregnated with resin in a vacuum, air-dried again, then cut with a diamond saw and finally polished for microscopic observations.

3.2.2. Physical and Chemical Analysis

The physical and physico-chemical analyses were done at the International Institute for Tropical Agriculture (IITA) at Nkolbissong, Yaoundé. So, bulk density (Bd) was determined in reference to Archimedes' principle [20]. Particle size

distribution was measured by Robinson's pipette method [20]. The pH-H₂O was determined in a soil/H₂O ratio of 1:2 and pH-KCl in a soil/KCl ratio of 1: 2 using a glass pH meter [34]. The presence of carbonates was tested with dilute HCl solution. The organic carbon (OC) was measured by Walkley-Black procedure [40]. The organic matter was deduced from the Springel's coefficient [20]. Total nitrogen (TN) was measured by the Kjeldahl method [7]. Available phosphorus was determined by concentrated nitric acid reduction method [47]. Exchangeable cations were dosed by ammonium acetate extraction method and cation exchange capacity (CEC) was determined using the sodium saturation method [60].

3.2.3. Clay Mineralogy Analysis

X-ray diffraction (XRD) analysis was first performed on

non-oriented powder of the dried total fraction. This was done using a Bruker AXS model D8 Advance diffractometer, with Cu-K α radiation, under 40 kV and 30 mA operating conditions. The XRD patterns were recorded over the 2°- 45°2 θ angular range using a step scan 0.02°2 θ and a step time of 2 seconds. Additional measurements were performed on oriented aggregates [35] prepared from the < 2 μ m fraction obtained by suspension in distilled water of 1 – 2 g of the bulk clay samples. The suspension was first sieved at 63 μ m to limit particle settling during decantation. The sieving also reduced the amount of impurities within the clay aggregates.

The < 2 μ m fraction is taken from the suspension after a settling time calculated according to Stock's law, placed on a glass slide and the XRD patterns were thus recorded between 2° and 30°2 θ using the same step size and time per step parameters. These oriented aggregates were subjected to three successive treatments: air drying, glycolation and heating to 500°C for 4 hours, in order to confirm the nature of clay phases.

The Greene-Kelly test, modified by Lim and Jackson [32] was also performed. To do so, the clay suspension was washed with 2N LiCl solution overnight. Samples were then rinsed with demineralized water, and prepared as oriented aggregates. XRD analyses on oriented clay mounts were conducted according to the following sequence: air-dried slide (N), heated at 300°C (H300, 2H), and finally overnight glycerol solvated (Gl). The Greene-Kelly test was carried out so as to characterize the swelling clay; in particular to differentiate smectites with tetrahedral substitution from those with octahedral substitution. After K-saturated of this < 2 μ m size fraction with 2N KCl solution, samples were then washed several times with demineralized water to remove chloride excess. XRD analyses on oriented clay mounts were performed successively in air-dried conditions (K-N), after heating to 110°C for 2 h (K-110), and after exchange with ethylene glycol (K-EG). K-saturation was done to identify the genetic conditions of the smectites [61].

The estimation of clay minerals contents in the soils samples was calculated using the equation defined by [64]:

$$T(x) = \sum MiPi(x) \quad (1)$$

where:

T(x) is the percentage of oxide of chemical element “x”;

Mi the percentage of mineral “i” in sample containing chemical element “x” and Pi(x) the proportion of element “x”

in mineral “i” (calculated from the ideal mineral formula). This calculation is based on the results of qualitative mineralogical identification of the samples. The quantification of smectite and kaolinite contents was performed on the basis of XRD and according to the method of Cook *et al.* [10].

First, the relative content of clay minerals (smectite + kaolinite) was estimated from the relative intensity of the peak at 4.47 Å on the XRD patterns obtained for the < 2 μ m fractions. In a second step an estimate of the relative proportion of smectite and kaolinite was obtained from the relative (001) reflection intensities for these two clay minerals on the XRD patterns obtained for the < 2 μ m fractions (glycolated specimens). The related error for this calculation is estimated at 10%.

3.2.4. Geochemical Analysis

Geochemical analyses were carried out using emission spectrometry (Nancy, France). Approximately 1g of soil powder was molded in fused lithium borate (LiBO₂) and dissolved in nitric acid. Inductive Coupled Plasma by Atomic Emission Spectrometry (ICP-AES) was used for the determination of major elements and Inductive Coupled Plasma by Mass Spectrometry (ICP-MS) was used for trace elements. Major elements determined by ICP-ES were SiO₂, Al₂O₃, Fe₂O₃, MnO, MgO, CaO, Na₂O₃, K₂O, TiO and P₂O₅. Relative analytical uncertainties were estimated at 1 – 5% for major elements except for P₂O₅ (10%). The results helped to evaluate the degree of weathering using the Chemical Index of Alteration (CIA) as developed by [41]:

$$CIA = [Al_2O_3 / (Al_2O_3 + CaO^* + Na_2O + K_2O)] \times 100 \quad (2)$$

where, CaO* is the CaO incorporated in silicate minerals of the rock, while Na₂O, K₂O and Al₂O₃ are base concentrations from the soil sample.

Trace and rare earth elements were determined by ICP-MS: ⁷⁵As, ¹¹Ba, ⁹Be, ²⁰⁹Bi, ¹¹⁴Cd, ¹⁴⁰Ce, ⁵⁹Co, ⁵²Cr, ¹³³Cs, ⁶³Cu, ¹⁶⁴Dy, ¹⁶⁶Er, ¹⁵³Eu, ⁷¹Ga, ¹⁵⁸Gd, ⁷⁴Ge, ¹⁸⁰Hf, ¹⁶⁵Ho, ¹¹⁵In, ¹³⁹La, ¹⁷⁵Lu, ⁹⁵Mo, ⁹³Nb, ¹⁴²Nd, ⁵⁸Ni, ²⁰⁸Pb, ¹⁴¹Pr, ⁸⁵Rb, ¹²¹Sb, ¹⁴⁷Sm, ⁸²Sn, ⁸⁸Sr, ¹⁵⁹Ta, ²³²Th, ¹⁶⁹Tm, ²³⁸U, ⁵⁰V, ¹⁸⁴W, ⁸⁹Y, ¹⁷⁴Yb, ⁶⁶Zn and ⁹⁰Zr. They were up to 5% for most of the trace element concentrations except for Cu (10%). However, uncertainty was high (> 10%) for any trace element displaying a low concentration (< 0.1ppm). REE concentrations were normalized to chondrite [50] and have allowed calculating [46] the following values:

$$Ce/Ce^* = (Ce_{sample}/Ce_{chondrite}) / (La_{sample}/La_{chondrite})^{1/2} (Pr_{sample}/Pr_{chondrite})^{1/2} \quad (3)$$

$$Eu/Eu^* = (Eu_{sample}/Eu_{granite}) / (Sm_{sample}/Sm_{granite})^{1/2} (Gd_{sample}/Gd_{granite})^{1/2} \quad (4)$$

$$(La/Yb)_N = (La_{sample}/La_{chondrite}) / (Yb_{sample}/Yb_{chondrite}) \quad (5)$$

$$(La/Sm)_N = (La_{sample}/La_{chondrite}) / (Sm_{sample}/Sm_{chondrite}) \quad (6)$$

$$(Gd/Yb)_N = (Gd_{sample}/Gd_{chondrite}) / (Yb_{sample}/Yb_{chondrite}) \quad (7)$$

3.3. Statistical Analysis

Results were assessed by descriptive statistics, including

Pearson's correlation coefficient (r) (with significance levels at p < 0.05) and principal component analysis. The basic statistical parameters for each element and the statistical

calculations were performed using the statistical software program XLSTAT and Statistica VI.

4. Results and Discussion

4.1. Pedological Characteristics of Vertisols

4.1.1. Soil Profile Descriptions

(i). Lowland Vertisols

The most representative lowland Vertisols are observed in Ndiguina located between 11°49'N and 14°27'E (Table 1). The profile is located in a low zone with an altitude of 299 m and slightly concave, along a temporary stream. The material is formed on alluvium. A very well marked gilgai micro-relief covers the entire surface. The profile is approximately 5 m deep. From top to bottom, we observe (Table 2A).

(ii). Upland Vertisols

Upland Vertisol is described in Kaele located between 10°01'52"N and 14°19'36"E latitude. The profile is located at 300m altitude. At the surface, a gilgai "microrelief" with unevenness of the order of 50 cm thick develops. The 3 m thick soil is developed on granite. From top to bottom, we observe (Table 2B).

4.1.2. Macromorphological Characteristics, Field Observation and Classification

Lowland Vertisols have a less coarse structure in depth; the tendency to prismatic structuring present in the profile of the upland Vertisols does not appear in the profile of the Lowland Vertisols (Figure 2A and B). There is also a thicker profile in the lowland Vertisols with a more marked hydromorphic along the profile. This difference may be due to the difference in humidity; lowland Vertisols have higher humidity, cool horizons to the surface, while in upland Vertisols the upper horizons are dry.

Vertisols studied were characterized by a gray to dark gray color, a clayey texture and deep open surficial desiccation cracks, but also by the development of frictional surfaces (slickensides) in the middle part of the profile (Table 2). The color of the studied Vertisols is gray to dark gray and range between 2.5Y and 10YR in the Munsell Color Charte (Table 2). Lowland Vertisols have dark-colored surface and there is no change in color throughout the profile. Despite the fact that their total organic matter content is relatively low, their dark color, common to Vertisols, can be attributed to the complexation or chelation of organic colloids with smectite [30]. The dark color (low chroma) could be related to the strong impregnation of the whole profile by organic matter during pedogenesis or to prolong waterlogging [24]. The low chromas are commonly used to predict seasonal variations and are characteristic of hydric soils [15].

Cracks and micro relief gilgai are most present at the surface of the soils and slickensides are described within the profiles. The presence of cracks can be explained by the capacity of Vertisols to swell and shrink. According to

Hallsworth et al. [25], the development of gilgai is due to the shrinking and swelling of the Vertisols. On wetting and swelling, the soil mass cannot re-occupy the original volume since surficial material has fallen into the cracks during the dry season. As such, part of the soil mass is forced upwards forming the mounds [59, 29]. According to Coulombe et al. [11] the formation of gilgai would proceed as follows: (i) formation of deep cracks during the dry period, (ii) upon rewetting a dry soil, the wetting front moves from the bottom of the cracks to the surface and the cracks close, (iii) slickensides are formed and induce the formation of thrust cones due to the polygonal network of cracks, (iv) formation of these thrust cones forces the soil to move up inducing a slightly undulating topography, and (v) the topography is amplified by drying-wetting cycles and/or differential leaching.

The formation of slickensides requires the material to be in a plastic state [18]. During the drying periods, cracks develop, whereas, on moistening, shear stresses form which result in slickensides. Kovda et al. [29] noted that the formation of these specific features, characteristics of Vertisols, are caused by a heavy texture, a dominance of swelling clays in the fine fraction and marked changes in moisture content. Such features are already been described in some Vertisols in North Cameroon [3, 59].

According to the Soil [56], the upland Vertisols is classified as Haplusterts and the lowland Vertisols as Endoaquerts.

4.1.3. Micromorphological Characteristics

According to microscopic descriptions (Figure 2a-i), in all horizons the plasma assemblage is insepic or epic with skeletal-voepsep tendencies. The epic plasmas fabric is observed in the lowland Vertisols (Figure 2a-e) meanwhile, insepic plasma is identified in the upland Vertisols (Figure 2f-i). The presence of the epic plasmic fabric may be explained by the fact that these soils are formed by the sedimentation processes and no muds development processes occurred [26, 58]. It is therefore identical to that of upland Vertisols. The porosity is essentially made up of subhorizontal and subvertical cracks. These two sets of characteristics would be specific to soils with moderately developed vertical characteristics. Micro-inclusions are also present in the horizons. Their constitution can hardly be demonstrated: they are coal debris, or opaque minerals. Some very few clay coatings are observed on the edges of the finest cracks. On the other hand, no coating integrated into the mass and deformed was highlighted. The absence of integrated coatings could be a sign of very slight clay movements in this profile, unlike upland Vertisols.

On the other hand, no matrane was observed, which may be due to the location of the thin blade collection. In the skeleton, there are on the one hand fragments of rock (in coarse sands) and on the other hand plagioclases (in silts) associated with grains of quartz. This material has a complex origin from colluvium or alluvium.

Table 2. Macro and micromorphological features of the paleosols from the Vertisols under tropical seasonally contrasted climate: (A) Lowland Vertisols and (B) Upland Vertisols.

A

Horizon	Depth (cm)	
Ap	0 – 80	Black (10 YR 2/0.5); fresh; clayey; fine and medium subangular and lumpy polyhedral structure, clean; low void volume between aggregates, consistent, few fine pore aggregates, low porosity horizon; numerous shiny faces; material with malleable consistency, non-friable, very plastic, sticky; many fine and medium roots between aggregates; regular transition.
Bss1	80–150	Black (10 YR 2/1); fresh; clayey; structure in oblique plates and fine polyhedral, clean; Very low void volume between aggregates, consistent, aggregates without visible pores; very little porous material; presence of slickensides, quite numerous; material with malleable consistency, non-friable, very plastic, very sticky; many fine and medium roots between aggregates; separate and regular transition.
Bss2	150–250	Black to very dark gray (10 YR 2.5 / 1); fresh; clayey; polyhedral structure and in medium and coarse oblique plates, with polyhedral substructure and in fine and very fine oblique plates; very low void volume between aggregates, consistent, aggregates without visible pores; very little porous material; presence of slickensides, very numerous; material with malleable consistency, non-friable, very plastic, very sticky; fine and medium roots between the aggregates and penetrating the aggregates; separate and regular transition.
Bssck1	250–380	Black to very dark greyish brown (7.5 YR 2.5/1.5); clayey; polyhedral structure and oblique plates, fine and medium; weak localized effervescence, less than 2% of carbonate elements in nodules; very low void volume between aggregates, consistent, aggregates without visible pores; very little porous; presence of slickensides; material with malleable consistency, non-friable, very plastic, very sticky; some fine roots, mostly rotten: regular transition.
Bssck2	380–430	Dark brown material (7.5 YR 3.5/3); fresh; numerous yellowish red (5 YR 4/8) and brown to pale brown (10 YR 5.5/3) spots sparse, in aggregates, rounded; clay; polyhedral structure and oblique plates, coarse and medium, with polyhedral substructure; approximately 20% of slightly altered and weathered irregularly shaped gravel; lively widespread effervescence; very low void volume between aggregates, consistent, aggregates without visible pores; not very porous; presence of slickensides; semi-rigid, not very brittle, slightly plastic, sticky material; some fine and rotten roots; regular transition.
Bck	430–500	Reddish brown (5 YR 4/4); fresh; some spots, red (2.5 YR 4/8), rounded, 1 to 2 mm in diameter, edges not very clear, not very contrasted; silty clayey; approximately 60% of irregularly shaped, slightly weathered and weathered gravel; poorly defined medium polyhedral structure; very little porous material; semi-rigid, brittle, plastic, slightly tacky material; no roots.

B

Horizon	Depth (cm)	
A1	0–20	Black (10 YR 2/1); dry; silty clay; fine, very distinct subangular polyhedral structure; fairly large void volume between the aggregates, aggregates with few pores, very fine, not very porous horizon; material with semi-rigid consistency, not very fragile, not very plastic, not very sticky in the wet state; many fine roots between the aggregates; regular transition.
A2	20–50	Black (10 YR 2/0.5); dry; silty clay; medium to coarse subangular polyhedral structure with very clear prismatic structure; low void volumes between aggregates, consistent, 1 to 2 cm wide and 20 cm distance recesses, few pore aggregates, thin, tubular; not very porous; rigid, non-brittle, plastic, sticky material; many fine roots between the aggregates; gradual and regular transition.
Bss	50–150	Dark gray to black (5 YR 2.5/1); fresh; few sparse spots, dark brown (7.5 YR 3/2), irregular, with sharp boundaries, very contrasting, sizes of 1 mm; clay; prismatic structure, with very distinct oblique platelet structure; low void volumes between aggregates, consistent, no shrinkage slots, aggregates without visible pores, very little porous; presence of slickensides; material with malleable consistency, very plastic, very sticky, non-friable; some fine roots between the aggregates; gradual and regular transition.
Bck	150–220	Dark gray (5 YR 2.5/1); fresh; without stains; clay; prismatic structure, with very distinct oblique platelet structure; generalized effervescence, 2 to 5% of carbonate elements in nodule (1 to 2 mm in diameter); very low void volume between aggregates, consistent, with no visible pores; very little porous; presence of slickensides; material with malleable consistency, plastic, very sticky, non-friable; no root; gradual and regular transition.
C	220–300	Gray (2.5 YR 3.5/3); fresh; clay-sandy; coarse, clean polyhedral structure; very low void volume between aggregates, aggregates without visible pores, consistent; very little porous; material with a semi-rigid consistency, non-friable and not very sticky; no roots; gradual transition with the source rock (granite).
R	> 300	Granite.

The different horizons are therefore characterized by a lightly colored groundmass, with a yellowish aspect. Also, they show abundant and dense plasmas, with isotropic ones at the surface horizons and birefringent ones at depth, characterized by strong plasmic separations that mainly follow fissures. A less abundant heterogeneous skeleton comprised of smectites, quartz grains and opaque minerals are observed. Porosity is low, with voids mainly represented by few alveolar voids and a porphyric assemblage characterized by quartz grains, which are completely wrapped in the plasma.

According to Stoops *et al.* [58], differences in topography

can be ruled out and micromorphology sustains the field observation of an argic horizon with well-developed clay illuviation at the level of the fragipan at the deeper part of the profile which is not disturbed by bioturbation. De Carloa *et al.* [13] explain the difference in B horizons by different compositions of the clay fraction: in middle horizon, smectite is the dominant mineral, whereas at the surface trioctahedral chlorite and mica prevail are abundant. This could explain also why shrink-swell features (striated b-fabrics) occur throughout the B horizons in middle horizon, but are restricted to the deepest part of the horizons in the surface.

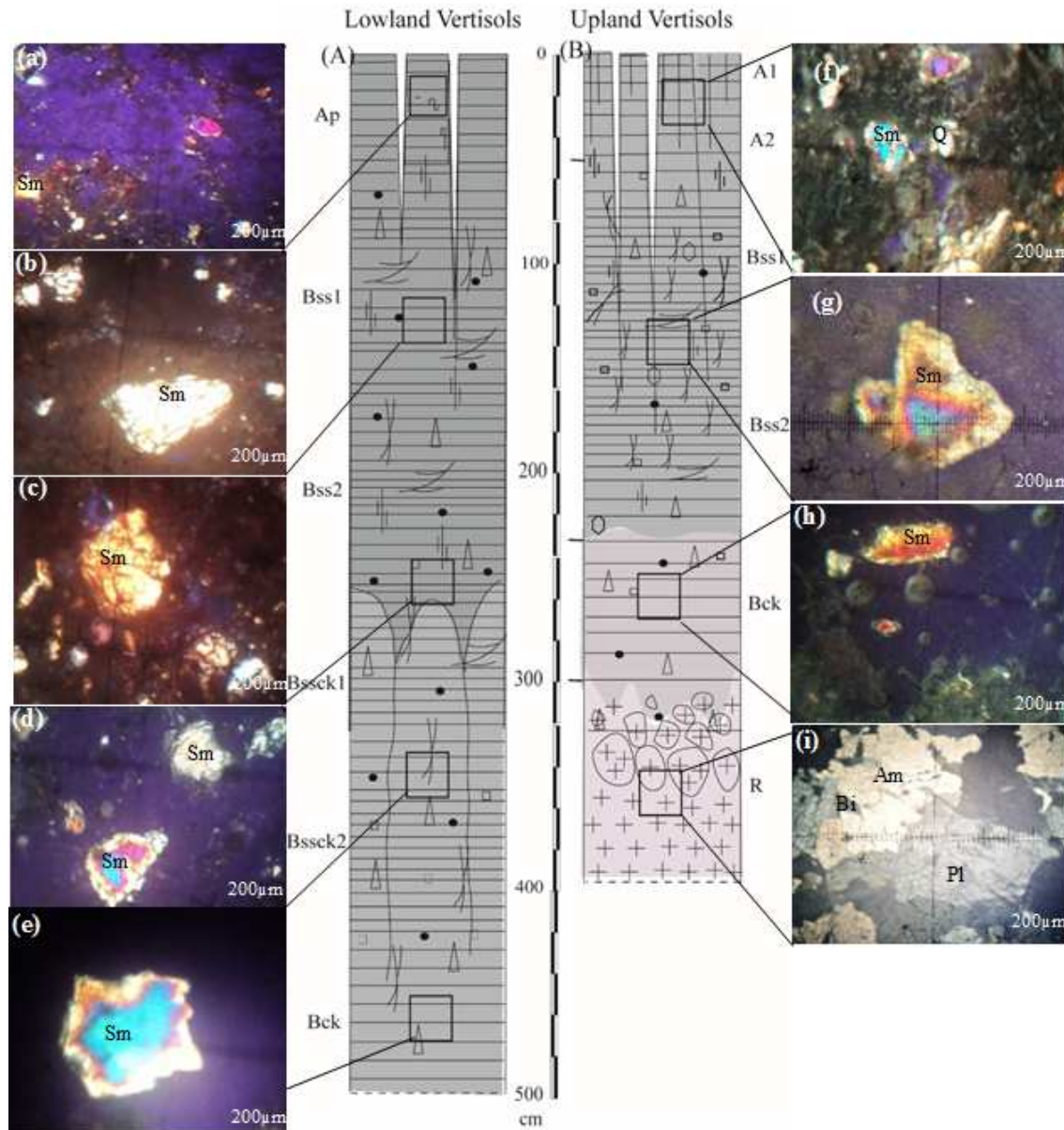


Figure 2. Macro and micromorphological features of the paleosols from the Vertisols under tropical seasonally contrasted climate: (A) Lowland Vertisols and (B) Upland Vertisols.

4.1.4. Physico-chemical Properties

A statistical summary of physico-chemical properties of the soils is given in Table 3. The grain size distribution analysis revealed that the clayey fraction ($0 - 2\mu\text{m}$) was most abundant in lowland Vertisols with mean value of 43.91% and ranged from 14.50 to 75.00%. The average clay content in Cameroon Vertisols are low compared with those of Thailand (61.62%, [9]), India (62.82%, [48]), Greece (50.21%, [36]), Ethiopia (63.06%, [66]) and Rusia (50.79%, [29]). The heavy clay texture of the lowland Vertisols could be associated to the low topographic position and the alluviation which is the principal process that brings sediments into the lower part of the watershed. Moreover, the observable increase in clay contents with depth could be related to slight eluviation-illuviation processes caused by downward movement of water through the

soil profiles leading to deposition of clay particles at deeper parts [36]. However, the highest sand contents were observed in upland Vertisols, with mean value of 48.46%. Silt contents have similar distribution, with mean value of 22.88% and 22.74% (Table 3), respectively in up- and lowland Vertisols.

Generally, the mean bulk density was very high, ranging from 1.7 to 2.2 (Table 3). It is slightly higher in lowland Vertisols, with mean value of 2.05 Mg m^{-3} .

The pH- H_2O ranged between 5.60 – 8.40 and 6.75 – 9.70 in lowland and upland Vertisols, respectively (Table 3). It revealed acidic to basic soils. The relatively more acidic pH values recorded for the present study, with respect to literature, could be justified by the absence of limestone in the soils. In addition, low pH could result from the presence of organic acids produced by plant roots, bacteria and fungi as well as aluminum hydrolysis [15]. The slightly lower trends observed

in the Benue floodplain could indicate a slow rate of weathering and soil development in the studied sites in relation to the continuous replenishment of alluvial parent material in this basin landform [1]. The seasonal flooding and the extensive water logging might also be contributing to the homogeneity [3].

The main characteristic that separates upland and lowland Vertisols is the rapid decrease in the rate of organic matter from the second horizon in the lowland Vertisols. The highest values were observed in upland Vertisols, with an average of 3.6% and the lowest ones in lowland Vertisols, with an average of 1.26 (Table 3). Differences in soil moisture at the start of the hot and dry season may explain this behavior. Indeed, the lowland Vertisols, because of its situation in the shallows, stays wet longer than the upland Vertisols, allowing a more intense biological activity and a greater destruction of organic matter. In the other hand, higher organic matter at the upland Vertisols could be linked to the continuous addition of crop residues on the surface of cropped fields in the area [5]. Moreover, the low content in organic matter at the lowland could be explained by variation in periods of flooding, since long flooding periods maintain organic matter wet and so decrease mineralization [3].

Total nitrogen contents varied from 0.1 to 0.02%. These values decrease from the top to the bottom in Vertisols profiles (Table 3). Total available phosphorus varied between 0.54 and 81.20 ppm in lowland Vertisols (Table 3). The upland Vertisols had slightly high Ca^{2+} contents (0.20 to 15.08 Cmol.kg^{-1}) while those of lowland Vertisols were relatively higher in Mg^{2+} with value ranging from 3.69 to 31.84 Cmol.kg^{-1} (Table 3). The higher values of total nitrogen and available phosphorus alongside the soil organic matter in surficial horizons and a subsequent decline with depth indicated that the nitrogen and phosphorus were largely associated with soil organic matter which disappeared through rapid decomposition mediated by microbes and abiotic processes [2].

Calcium was the dominant exchangeable cation, with contents ranging between 15.20 and 26.60 Cmol.kg^{-1} , which was about 60 to 70% of total bases. Calcium is the most abundant element in Vertisols observed in countries as Thailand (45.80 Cmol.kg^{-1} , [9]), India (37.42 Cmol.kg^{-1} , [49]), Greece (29.66 Cmol.kg^{-1} , [36]), Ethiopia (28.92 Cmol.kg^{-1} , [63]) and Russia (25.3 Cmol.kg^{-1} , [29]).

The cation exchange capacity varied from 26 to 42 Cmol.kg^{-1} , and generally increases from the surface to the base of the profiles. The cation exchange capacity was very high and perhaps correlated with the high smectite contents imposed by low topography, strongly contrasted climate and the presence of a clay-rich alluvial parent rock [3, 59]. Those high values indicated high fertility potentials since high cation exchange capacity implies the capacity to retain nutrients of added fertilizers [2].

Base saturation (S/T) globally fluctuated from 74.30 to 94.23% (Table 3) and confirmed that the absorption complex was highly saturated with exchangeable bases; the incomplete base saturation values, revealed the presence of exchangeable H^+ and/or Al^{3+} responsible for pH value of those Vertisols. The

high base saturation was related to the low topographic position and the contrasted tropical climate with a well-marked dry season; those factors are favorable for the synthesis and conservation of smectite which is the main colloid responsible for cation adsorption in Vertisols [2, 3, 30]

4.2. Mineralogical Properties

The mineralogical analysis revealed that smectite and interstratified kaolinite-smectite were the most abundant mineral component in upland (63.94%) and lowland (75.79%) Vertisols. It was associated with kaolinite and to small proportions of illite, quartz and feldspars (Table 3). The results of the ethylene glycol test on one sample showed a characteristic displacement of the principal peak of smectite (Figure 3a and b). It is characterized by a high intense peak, which indicates a very good crystallinity. This peak is between 14.7 - 14.9 Å (N), swells around 16.9 - 17.3 Å after treatment with ethylene glycol (EG), and crashes at 9.9 Å after heating at 550°C (CH). Kaolinite also has a very intense peak and is located at 7.108 - 3.559 - 1.452 Å in the normal state (N) and after treatment with ethylene - glycol (EG). It disappears after heating to 550°C (CH). Smectites-kaolinite interstratified is materialized by an irregular set of badly crystallized peaks lower than 14 Å in normal plate. These minerals swell after treatment with ethylene glycol and disappear after heating. Finally, quartz (reflection at 4.242 - 3.335Å) mainly and feldspars (reflection at 3.476 - 3.232Å) incidentally, were also detected in the fine fraction and accompany the clay minerals in all the samples. The peak for mica was not very sharp (1.0 nm), indicating that illite was the initial mica weathering product [54]. The persistence of this peak after ethylene glycol solvation treatment confirms the presence of illite in the upland Vertisols.

4.3. Geochemistry

4.3.1. Major Element Distribution in Vertisols

Silicon, aluminium and iron are the most abundant elements in lowland and upland Vertisols (Table 4). Silicon contents were highest and ranged from 49.56 to 74.52% SiO_2 at upland Vertisols, and lowest at lowland Vertisols (50.31 to 50.81% SiO_2). The aluminium contents ranged between 9.97 to 22.58% Al_2O_3 and 1.66 to 23.74% Al_2O_3 in lowland and upland Vertisols, respectively (Table 4). Bases were also present, with average ranged from 1.11 - 3.07% CaO , 0.62 - 2.52% Na_2O , 1.43 - 1.88% K_2O and 0.81 - 0.82% MgO which are most represented in upland Vertisols (Table 4). Manganese and phosphorus were negligible, with 0.07% MnO and 0.05 - 0.07% P_2O_5 (Table 4). Manganese was the least represented base in upland Vertisols, while phosphorus was the least represented in lowland Vertisols. Alkaline and alkali-earth elements which were uniformly distributed throughout the Vertisols were probably related to the low topographic position and the strongly contrasted climate which limit leaching rate and moderates lixiviation [2]. The presence of calcareous nodules is responsible for high CaO contents and dolomite lead to the increase of MgO contents. The Harker diagrams indicate slight

negative correlations between Si and Al, Fe, and Ti (MgO and CaO) show no correlation with silica (Figure 4a-d). The alkali (Na₂O and K₂O) and alkali-earth (4e-h).

Table 3. Statistical summary of some physico-chemical properties of Cameroon Vertisols compared to international Vertisols data.

Soil property	Lowland Vertisols (n=48)				Upland Vertisols (n=35)			
	Mean	Max	Min	SD	Mean	Max	Min	SD
<i>Physical properties</i>								
Clay (< 2µm), (%)	43.91	75.00	14.50	16.22	27.26	48.00	7.62	12.02
Silt (2 – 50 µm), (%)	22.84	35.00	5.00	6.35	22.74	36.24	6.35	6.84
Sand (50 – 200 µm), (%)	31.54	74.00	6.30	18.12	48.46	86.02	18.00	16.18
Bulk density (Mg m ⁻³)	2.05	2.2	1.8	0.15	1.95	2.1	1.7	0.25
<i>Chemical properties</i>								
pH (1: 1 H ₂ O)	7.25	8.40	5.60	0.72	8.09	9.70	6.75	1.20
pH (KCl)	6.08	7.30	4.00	0.76	6.63	7.60	5.57	0.73
Carbon organic, (g kg ⁻¹)	0.94	3.47	0.26	0.72	1.92	3.52	0.77	0.76
Organic matter, (g kg ⁻¹)	1.26	4.50	0.62	0.82	3.60	7.08	1.33	1.65
Total Nitrogen, (g kg ⁻¹)	0.21	1.34	0.02	0.33	0.38	0.59	0.13	0.12
Available P, (g kg ⁻¹)	14.38	81.20	0.54	17.71	-	-	-	-
Exchangeable Ca ²⁺ , (Cmol kg ⁻¹)	19.20	31.84	3.69	7.76	4.29	15.08	0.20	5.60
Exchangeable Mg ²⁺ , (Cmol kg ⁻¹)	5.00	11.60	0.00	3.96	15.23	54.45	1.12	14.52
Exchangeable Na ⁺ , (Cmol kg ⁻¹)	0.56	1.88	0.01	0.57	0.11	0.61	0.04	0.17
Exchangeable K ⁺ , (Cmol kg ⁻¹)	0.48	2.80	0.02	0.65	0.07	0.84	0.15	0.24
Base saturation, (%)	26.96	52.24	13.28	10.51	19.84	57.77	7.65	12.05
CEC, (Cmol kg ⁻¹)	25.92	46.00	2.67	12.70	23.84	39.84	12.80	7.68
C/N	18.09	34.75	2.67	7.65	5.43	8.80	0.48	2.67
S/CEC	59.05	260.12	0.74	76.71	80.65	267.40	0.36	66.92
<i>Mineralogical properties</i>								
Smectites (Sm)	33.91	77.14	9.10	20.56	53.99	100.00	24.60	23.99
Kaolinite (Kao)	23.10	119.18	2.53	24.59	10.35	30.44	2.18	6.38
Kao-Sm	41.24	60.66	1.92	17.24	24.30	45.87	0.00	16.06
Illite (Il)	9.32	15.54	1.17	5.42	-	-	-	-
Quartz (Q)	8.26	25.64	1.77	5.07	11.94	28.86	4.00	6.92
Feldspar (Fe)	1.70	2.77	0.98	0.53	3.12	7.15	1.06	2.75

Table 3. Continued.

Soil property	Thailand ^a (n=98)	India ^b (n=6)	Greece ^c (n=18)	Ethiopia ^d (n=18)	Russia ^e (n=8)
	Mean±SD	Mean±SD	Mean±SD	Mean±SD	Mean±SD
<i>Physical properties</i>					
Clay (< 2µm), (%)	61.62±15.5	62.82±2.40	50.21±4.63	63.06±15.38	50.79±12.08
Silt (2 – 50 µm), (%)	23.13±9.6	35.81±1.87	34.91±2.09	-	36.8±6.51
Sand (50 – 200 µm), (%)	15.01±13.4	1.37±0.65	15.08±5.69	-	12.41±7.49
Bulk density (Mg m ⁻³)	1.75±0.14	1.5±0.5	-	-	1.39±0.17
<i>Chemical properties</i>					
pH (1: 1 H ₂ O)	7.65±0.85	8.18±0.32	7.86±0.28	6.78±0.81	7.46±1.02
pH (KCl)	-	-	-	5.11±0.66	-
Carbon organic, (g kg ⁻¹)	11.40±9.12	0.6±0.14	-	1.03±0.70	1.05±1.20
Organic matter, (g kg ⁻¹)	-	-	0.49±0.21	-	-
Total Nitrogen, (g kg ⁻¹)	0.45±0.40	-	-	0.11±0.06	0.20±0.18
Available P, (g kg ⁻¹)	6.55±21.20	-	-	1.10±0.73	-
Exchangeable Ca ²⁺ , (Cmol kg ⁻¹)	45.80±19.60	37.42±8.27	29.66±12.35	28.92±10.01	25.3±5.46
Exchangeable Mg ²⁺ , (Cmol kg ⁻¹)	6.58±6.34	18.73±3.34	4.99±1.55	6.95±1.97	6.65±1.14
Exchangeable Na ⁺ , (Cmol kg ⁻¹)	1.59±1.98	4±2.87	0.19±0.02	1.40±0.57	1.41±1.10
Exchangeable K ⁺ , (Cmol kg ⁻¹)	0.11±0.07	0.8±0.2	0.64±0.34	2.53±0.81	0.91±1.10
Base saturation, (%)	76.70±9.59	60.8±2.6	-	78.12±13.27	29.37±14.28
CEC, (Cmol kg ⁻¹)	48.70±17.50	95±4.77	-	50.79±8.93	-
C/N	-	-	-	-	5.97±4.18

SD = Standard deviation; CEC = Cation exchange capacity

^a/ Mean concentration of physico-chemical properties in Thai Vertisols. Data are from Geoderma [9].

^b/ Mean concentration of physico-chemical properties of Vertisols of Peninsular India. Data are from Geoderma [49].

^c/ Mean concentration of physico-chemical properties of Vertisols in Greece. Data are from Catena [36].

^d/ Mean concentration of physico-chemical properties of Vertisols of the Bale Mountain area of Ethiopia. Data are from Tropicultura [63].

^e/ Mean concentration of physico-chemical properties of Vertisols of southern Siberia, Russia. Data are from Geoderma [30].

Table 4. Majors (wt.%), traces and rare earth (ppm) in the Vertisols with description statistics, compared to results from: Ferralsols [4], Lixisols [4] and Andosols [19].

Oxides	D.I	Upland Vertisols (n=55)				Lowland Vertisols (n=82)			
		Meen	Max	Min	SD	Mean	Max	Min	SD
SiO ₂	0.04	65.03	74.52	49.56	6.25	64.00	85.06	46.37	9.74
Al ₂ O ₃	0.02	14.72	22.58	9.97	2.53	14.35	23.74	1.66	4.98
Fe ₂ O ₃	0.1	4.34	8.65	0.79	1.56	4.94	8.94	0.83	2.03
MnO	0.01	0.07	0.20	0.00	0.04	0.07	0.24	0.01	0.04
MgO	0.02	0.82	2.86	0.17	0.64	0.81	2.80	0.08	0.57
CaO	0.01	3.07	12.00	0.05	2.19	1.11	4.74	0.20	0.72
Na ₂ O	0.01	2.52	6.84	0.57	1.31	0.62	1.88	0.07	0.42
K ₂ O	0.01	1.43	3.70	0.48	0.81	1.88	3.26	0.23	0.57
TiO ₂	0.01	0.66	1.26	0.07	0.22	0.98	2.46	0.15	0.33
P ₂ O ₅	0.01	0.50	4.80	0.01	1.16	0.07	0.21	0.00	0.06
LOI	0.05	6.67	13.77	1.30	2.80	9.47	18.15	1.54	3.52
Total		99.95	101.10	97.89	0.49	98.26	108.17	61.65	6.91
CIA		64.80	78.48	44.27	9.62	77.34	92.13	54.66	7.78
Ba	0.8	506.99	1454.00	176.00	231.06	851.54	1069.00	476.20	150.77
Be	0.04	2.18	3.98	1.53	1.20	2.70	3.90	1.64	0.57
Bi	0.15	0.13	0.19	0.09	0.03	0.21	0.39	0.11	0.07
Cd	0.01	0.36	0.48	0.30	0.06	0.43	0.78	0.31	0.15
Co	0.13	14.21	22.85	3.41	5.00	17.51	34.48	6.59	7.01
Cr	3	524.95	721.20	129.00	168.57	513.33	812.30	195.90	147.96
Cs	0.01	1.00	1.80	0.22	0.47	2.86	5.18	1.52	0.79
Cu	1.4	32.23	128.60	5.73	30.25	27.62	41.81	15.02	7.17
Ga	0.4	18.10	25.93	12.60	3.61	22.81	33.27	14.67	4.83
Hf	0.14	7.58	12.62	1.95	3.44	12.61	32.62	5.28	5.69
In	0.01	0.06	0.06	0.06	0.03	0.12	0.13	0.10	0.01
Mo	0.08	5.89	8.91	1.25	2.04	5.41	8.51	1.86	1.57
Nb	0.03	8.84	22.42	0.86	4.54	20.65	32.26	12.51	5.76
Ni	1.6	28.15	41.20	10.06	7.96	42.76	68.03	16.48	14.39
Pb	0.03	10.50	17.18	3.88	4.39	25.14	32.94	20.53	3.46
Rb	0.23	43.45	76.00	10.06	18.25	101.09	135.10	70.19	17.66
Sb	0.04	0.31	1.51	0.10	0.30	0.25	0.62	0.14	0.09
Sn	0.16	2.44	3.46	1.33	0.59	4.18	5.24	3.14	0.57
Sr	0.6	453.87	1073.00	110.40	260.33	165.95	253.50	76.66	37.52
Ta	0.02	0.73	1.55	0.06	0.39	1.81	2.70	1.17	0.47
Th	0.02	4.80	10.18	0.50	3.35	18.88	23.18	12.49	2.89
U	0.01	1.60	3.79	0.27	0.98	3.91	5.45	2.34	0.70
V	0.8	81.54	172.70	16.81	33.49	85.45	133.90	45.04	25.27
W	0.05	23.33	32.51	4.82	7.77	21.13	34.37	6.10	7.20
Y	0.05	19.49	47.99	2.11	8.65	30.71	44.34	18.31	5.64
Zn	7	46.85	82.61	11.29	19.40	58.44	95.91	33.17	18.74
Zr	6	295.80	513.00	59.83	13.21	496.48	1339.00	204.90	235.70
La	0.04	23.30	37.29	4.41	7.86	56.56	96.06	26.29	16.45
Ce	0.12	52.01	75.75	11.64	19.20	120.14	222.90	70.85	34.62
Pr	0.014	6.16	9.07	1.19	1.90	13.16	20.87	6.74	3.41
Nd	0.06	24.15	35.34	4.53	7.12	47.79	77.13	24.18	12.68
Sm	0.012	4.77	8.03	0.85	1.43	8.66	13.27	4.67	2.12
Eu	0.0031	1.21	1.76	0.44	0.28	1.76	2.92	0.91	0.49
Gd	0.009	3.98	7.31	0.61	1.29	6.78	10.53	3.73	1.63
Tb	0.0023	0.59	1.28	0.07	0.22	0.98	1.48	0.55	0.22
Ho	0.009	0.66	1.54	0.07	0.28	1.05	1.54	0.61	0.21
Dy	0.0025	3.41	7.87	0.37	1.37	5.49	7.94	3.20	1.13
Er	0.007	1.89	4.78	0.21	0.85	2.96	4.08	1.83	0.51
Tm	0.0019	0.28	0.73	0.03	0.13	0.45	0.62	0.28	0.08
Yb	0.009	1.95	4.93	0.22	0.92	3.06	4.16	1.95	0.49
Lu	0.002	0.31	0.74	0.04	0.14	0.48	0.63	0.33	0.07
REE		137.50	313.25	24.70	56.05	275.64	463.76	148.24	72.60
LREE		123.71	291.73	23.06	51.75	254.03	433.15	133.76	68.41
HREE		13.79	29.17	1.63	5.23	21.62	30.61	12.48	4.38
LREE/HREE		8.97	10.00	14.13	9.90	11.75	14.15	10.72	15.63
Ce/Ce*		1.07	1.36	0.62	0.17	1.05	1.29	0.91	0.09
Eu/Eu*		0.88	1.87	0.36	0.27	0.71	0.75	0.59	0.04
(La/Yb)N		8.78	13.69	4.46	2.19	13.04	17.13	7.38	2.30
(La/Sm)N		3.13	3.93	2.12	0.47	4.08	4.53	3.46	0.27
(Gd/Yb)N		1.72	2.33	1.14	0.35	1.86	2.24	1.37	0.22

Table 4. Continued.

Oxides	Ferralsol (n=10) ^a		Lixisols (n=10) ^b		Andosols (n=11) ^c	
	Mean	SD	Mean	SD	Mean	SD
SiO ₂	53.75	9.80	51.81	4.17	27.87	4.43
Al ₂ O ₃	14.31	12.10	16.88	1.56	22.34	2.59
Fe ₂ O ₃	16.94	4.93	11.22	3.49	15.42	2.43
MnO	0.04	0.02	0.20	0.14	0.38	0.10
MgO	0.84	0.51	1.89	1.25	2.03	1.58
CaO	0.06	0.04	1.83	1.04	4.31	3.89
Na ₂ O	0.03	0.02	5.70	5.56	0.37	0.71
K ₂ O	2.65	1.90	1.03	0.99	0.33	0.37
TiO ₂	1.09	0.35	1.38	0.25	4.86	0.95
P ₂ O ₅	0.07	0.03	0.20	0.08	0.73	0.25
LOI	-	-	7.06	2.16	21.57	7.82
Total	99.68	0.72	99.26	0.75	100.21	0.12
CIA	79.35	13.91	68.51	11.48	82.83	13/64
Ba	-	-	367.63	191.70	2067.60	604.81
Be	-	-	1.14	0.50	-	-
Bi	-	-	-	-	-	-
Cd	-	-	-	-	-	-
Co	-	-	49.19	28.78	42.04	11.11
Cr	-	-	246.70	126.94	34.12	30.14
Cs	-	-	29.51	7.65	1.49	0.84
Cu	-	-	108.55	50.18	128.37	50.11
Ga	-	-	20.26	3.49	33.12	6.92
Hf	-	-	9.33	9.41	14.35	2.70
In	-	-	-	-	-	-
Mo	-	-	1.94	2.24	-	-
Nb	-	-	6.59	2.32	362.90	135.35
Ni	-	-	103.52	38.45	26.52	16.07
Pb	-	-	9.84	9.84	11.02	3.77
Rb	-	-	21.61	20.19	24.95	32.85
Sb	-	-	-	-	-	-
Sn	-	-	-	-	-	-
Sr	-	-	246.51	124.88	1331.23	789.59
Ta	-	-	73.24	137.33	23.22	8.22
Th	-	-	1.41	0.70	-	-
U	-	-	75.28	116.88	-	-
V	-	-	230.49	43.90	372.55	62.90
W	-	-	-	-	-	-
Y	-	-	25.04	6.74	56.90	17.81
Zn	-	-	88.90	21.05	218.61	50.26
Zr	-	-	92.40	34.33	805.04	205.21
La	19.55	9.15	11.22	4.03	280.51	115.56
Ce	45.80	25.28	36.78	25.88	562.12	193.15
Pr	4.23	1.94	3.66	1.06	55.41	18.28
Nd	14.47	6.52	16.85	4.85	189.46	58.36
Sm	2.60	1.10	4.18	1.15	26.50	7.11
Eu	0.52	0.20	1.43	0.43	7.65	1.98
Gd	2.14	0.80	4.45	1.23	17.79	4.40
Tb	0.42	0.14	0.70	0.19	2.51	0.65
Ho	0.75	0.26	0.91	0.23	2.12	0.59
Dy	3.21	1.09	4.54	1.19	12.50	3.32
Er	2.41	0.83	2.71	0.67	5.55	1.62
Tm	0.36	0.12	0.39	0.09	0.74	0.20
Yb	2.40	0.82	2.52	0.54	4.47	1.29
Lu	0.35	0.12	0.37	0.08	0.61	0.18
REE	99.22	46.05	90.71	28.35	1167.94	400.31
LREE	87.17	42.67	74.12	27.55	1121.65	389.30
HREE	12.04	4.02	16.59	4.21	46.28	12.16
LREE/HREE	7.24	10.62	4.47	6.55	24.23	32.02
Ce/Ce*	1.51	1.40	1.20	0.19	1.10	0.08
Eu/Eu*	1.00	0.06	0.68	0.02	1.07	0.03
(La/Yb)N	2.99	0.61	5.48	1.38	41.87	10.17
(La/Sm)N	1.67	0.26	4.76	0.98	6.48	1.65
(Gd/Yb)N	1.41	0.13	0.73	0.11	3.26	0.26

D.I: Detection limite

Ce/Ce*: $(\text{Ce}_{\text{sample}}/\text{Ce}_{\text{chondrite}})/(\text{La}_{\text{sample}}/\text{La}_{\text{chondrite}})^{1/2}(\text{Pr}_{\text{sample}}/\text{Pr}_{\text{chondrite}})^{1/2}$.Eu/Eu*: $(\text{Eu}_{\text{sample}}/\text{Eu}_{\text{granite}})/(\text{Sm}_{\text{sample}}/\text{Sm}_{\text{granite}})^{1/2}(\text{Gd}_{\text{sample}}/\text{Gd}_{\text{granite}})^{1/2}$.(La/Yb)N: $(\text{La}_{\text{sample}}/\text{La}_{\text{chondrite}})/(\text{Yb}_{\text{sample}}/\text{Yb}_{\text{chondrite}})$.(La/Sm)N: $(\text{La}_{\text{sample}}/\text{La}_{\text{chondrite}})/(\text{Sm}_{\text{sample}}/\text{Sm}_{\text{chondrite}})$.(Gd/Yb)N: $(\text{Gd}_{\text{sample}}/\text{Gd}_{\text{chondrite}})/(\text{Yb}_{\text{sample}}/\text{Yb}_{\text{chondrite}})$.

Table 5. Pearson's correlation coefficients between REE, major elements and other important properties (sand, silt and clay contents, CEC, pH (H₂O), OM and CEC) in Vertisols under tropical seasonally contrasted climate (*n* = 111 soil samples).

Variables	%Clay	%Silt	%Sand	pHeau	%OM	CEC	La	Ce	Pr	Nd	Sm	Eu	Gd	Tb	Ho	Dy	Er
%Clay	1	-0.66	-0.83	0.53	-0.24	0.16	-0.28	-0.36	-0.29	-0.29	-0.27	-0.24	-0.32	-0.29	-0.37	-0.33	-0.41
%Silt	0.31	1	0.21	-0.41	-0.17	0.02	0.04	0.15	0.00	0.00	-0.05	0.03	0.01	-0.06	-0.05	-0.06	-0.04
%Sand	-0.93	-0.61	1	-0.38	0.55	-0.32	0.32	0.37	0.36	0.36	0.36	0.26	0.40	0.41	0.52	0.45	0.54
pH eau	0.38	0.13	-0.34	1	-0.24	-0.13	0.07	0.03	0.04	0.05	0.03	0.08	0.01	0.03	-0.04	-0.04	-0.09
%OM	-0.25	0.16	0.12	-0.54	1	-0.39	0.01	-0.02	0.04	0.03	0.03	-0.10	0.04	0.09	0.19	0.12	0.21
CEC	0.26	0.25	-0.30	0.45	-0.11	1	-0.27	-0.24	-0.21	-0.22	-0.16	-0.19	-0.19	-0.18	-0.17	-0.17	-0.17
La	0.21	-0.10	-0.20	0.16	-0.06	0.13	1	0.95	0.99	0.99	0.98	0.99	0.98	0.96	0.91	0.94	0.90
Ce	0.25	-0.05	-0.26	0.07	-0.01	0.06	0.91	1	0.95	0.95	0.94	0.95	0.96	0.94	0.91	0.93	0.90
Pr	0.17	-0.15	-0.15	0.13	-0.03	0.10	0.99	0.91	1	1.00	0.99	0.98	0.99	0.98	0.94	0.97	0.93
Nd	0.13	-0.24	-0.08	0.11	-0.06	0.17	0.91	0.83	0.93	1	0.99	0.99	0.99	0.98	0.94	0.97	0.93
Sm	0.13	-0.20	-0.11	0.09	0.01	0.08	0.91	0.83	0.96	0.92	1	0.98	0.99	0.99	0.96	0.98	0.95
Eu	-0.02	-0.30	0.08	0.13	-0.02	0.12	0.66	0.52	0.72	0.75	0.79	1	0.98	0.96	0.89	0.94	0.88
Gd	0.11	-0.24	-0.07	0.07	0.01	0.06	0.84	0.75	0.90	0.88	0.98	0.80	1	0.99	0.96	0.98	0.95
Tb	0.12	-0.25	-0.08	0.05	0.02	0.04	0.78	0.71	0.85	0.84	0.96	0.74	0.99	1	0.98	0.99	0.97
Ho	0.15	-0.26	-0.10	0.04	0.02	0.04	0.75	0.70	0.83	0.81	0.93	0.68	0.97	0.99	1	0.99	0.99
Dy	0.13	-0.25	-0.08	0.04	0.02	0.04	0.74	0.67	0.82	0.81	0.93	0.70	0.97	0.99	1.00	1	0.99
Er	0.14	-0.26	-0.10	0.03	0.02	0.03	0.71	0.65	0.79	0.77	0.90	0.63	0.95	0.98	1.00	0.99	1
Tm	0.15	-0.27	-0.11	0.02	0.01	0.02	0.70	0.66	0.78	0.76	0.88	0.61	0.93	0.96	0.99	0.98	0.99
Yb	0.14	-0.30	-0.09	0.02	0.01	0.02	0.70	0.66	0.78	0.76	0.88	0.62	0.92	0.96	0.98	0.97	0.99
Lu	0.15	-0.31	-0.09	0.02	0.01	0.02	0.70	0.65	0.77	0.75	0.87	0.62	0.91	0.94	0.98	0.96	0.98
REE	0.20	-0.13	-0.19	0.09	-0.02	0.09	0.96	0.96	0.97	0.92	0.93	0.67	0.87	0.84	0.81	0.80	0.77
LREE	0.21	-0.11	-0.20	0.10	-0.03	0.10	0.96	0.97	0.96	0.91	0.91	0.64	0.84	0.80	0.77	0.76	0.73
HREE	0.13	-0.26	-0.09	0.04	0.02	0.04	0.76	0.70	0.84	0.82	0.94	0.71	0.98	0.99	1.00	1.00	0.99
SiO ₂	0.22	0.00	-0.20	-0.18	0.07	-0.22	-0.07	0.03	-0.08	-0.19	-0.14	-0.50	-0.15	-0.07	0.02	-0.03	0.06
Al ₂ O ₃	-0.40	0.08	0.30	0.00	0.02	-0.02	-0.32	-0.29	-0.27	-0.18	-0.19	0.08	-0.16	-0.19	-0.25	-0.20	-0.25
Fe ₂ O ₃	-0.16	-0.23	0.22	0.03	-0.05	0.07	0.20	0.21	0.26	0.34	0.34	0.65	0.36	0.32	0.25	0.28	0.21
MnO	0.08	-0.20	0.02	0.10	-0.18	0.11	0.42	0.46	0.43	0.47	0.42	0.51	0.40	0.34	0.27	0.29	0.22
MgO	-0.48	-0.44	0.57	-0.01	0.02	0.01	0.02	-0.10	0.09	0.16	0.17	0.55	0.22	0.19	0.15	0.18	0.13
Na ₂ O	-0.16	0.04	0.16	0.26	-0.30	0.25	-0.11	-0.14	-0.12	-0.03	-0.09	0.03	-0.08	-0.11	-0.16	-0.12	-0.15
CaO	-0.27	-0.17	0.33	-0.05	-0.01	-0.05	-0.20	-0.42	-0.19	-0.10	-0.14	0.20	-0.09	-0.12	-0.17	-0.14	-0.18
K ₂ O	-0.15	-0.19	0.14	-0.04	0.08	-0.06	0.38	0.36	0.42	0.34	0.41	0.02	0.37	0.39	0.43	0.41	0.46
TiO ₂	-0.07	-0.07	0.07	0.00	-0.04	0.03	0.43	0.48	0.45	0.46	0.44	0.60	0.41	0.34	0.28	0.29	0.22
P ₂ O ₅	-0.18	0.31	0.04	-0.02	0.24	0.18	-0.26	-0.26	-0.28	-0.28	-0.33	-0.35	-0.33	-0.31	-0.29	-0.30	-0.29
CIA	0.52	-0.06	-0.43	0.11	0.00	0.11	0.47	0.50	0.47	0.44	0.47	0.57	0.46	0.43	0.41	0.40	0.37

Table 5. Continued.

Variables	Tm	Yb	Lu	REE	LREE	HREE	SiO ₂	Al ₂ O ₃	Fe ₂ O ₃	MnO	MgO	Na ₂ O	CaO	K ₂ O	TiO ₂	P ₂ O ₅	CIA
%Clay	-0.48	-0.43	-0.49	-0.33	-0.33	-0.36	0.11	-0.10	-0.16	-0.22	-0.22	-0.59	0.06	-0.56	-0.36	-0.67	0.39
%Silt	-0.02	-0.13	-0.04	0.08	0.08	-0.04	-0.13	0.08	0.18	0.29	0.29	0.29	0.00	0.16	0.34	0.46	-0.11
%Sand	0.64	0.65	0.68	0.37	0.36	0.49	0.01	0.02	-0.01	0.02	0.02	0.64	-0.02	0.68	0.19	0.50	-0.53
pH eau	-0.13	-0.15	-0.14	0.04	0.05	-0.04	-0.08	0.13	0.02	-0.59	-0.59	-0.09	0.05	0.01	0.12	-0.19	0.06
%OM	0.32	0.39	0.41	0.01	0.00	0.15	0.41	-0.30	-0.47	-0.15	-0.15	0.38	-0.22	0.57	-0.27	-0.02	-0.56
CEC	-0.16	-0.18	-0.23	-0.24	-0.24	-0.18	0.06	-0.15	-0.15	-0.03	-0.03	-0.24	0.55	-0.52	-0.36	-0.51	0.24
La	0.82	0.77	0.7	0.99	0.99	0.94	-0.78	0.79	0.81	0.23	0.23	-0.21	-0.07	-0.08	0.85	0.68	0.49
Ce	0.85	0.77	0.80	0.99	0.99	0.93	-0.73	0.74	0.77	0.35	0.35	-0.09	-0.13	-0.02	0.82	0.70	0.39
Pr	0.87	0.82	0.81	0.99	0.98	0.97	-0.78	0.78	0.78	0.22	0.22	-0.19	-0.02	-0.09	0.80	0.63	0.48
Nd	0.86	0.81	0.80	0.99	0.99	0.97	-0.78	0.79	0.79	0.22	0.22	-0.19	-0.02	-0.09	0.81	0.64	0.48
Sm	0.88	0.84	0.83	0.98	0.98	0.98	-0.78	0.78	0.77	0.22	0.22	-0.19	0.00	-0.11	0.77	0.59	0.48
Eu	0.80	0.73	0.72	0.98	0.98	0.93	-0.83	0.81	0.86	0.26	0.26	-0.26	0.01	-0.16	0.85	0.63	0.56
Gd	0.89	0.85	0.84	0.99	0.98	0.98	-0.77	0.77	0.77	0.27	0.27	-0.13	-0.01	-0.05	0.78	0.62	0.43
Tb	0.92	0.89	0.87	0.97	0.97	0.99	-0.77	0.79	0.71	0.19	0.19	-0.11	-0.02	-0.06	0.73	0.58	0.42
Ho	0.97	0.95	0.95	0.94	0.93	0.99	-0.69	0.72	0.61	0.20	0.20	0.03	-0.04	0.05	0.65	0.55	0.28
Dy	0.95	0.92	0.90	0.96	0.95	1.00	-0.75	0.77	0.69	0.22	0.22	-0.08	-0.01	-0.05	0.69	0.58	0.40
Er	0.98	0.96	0.95	0.93	0.92	0.99	-0.69	0.72	0.60	0.22	0.22	0.05	-0.05	0.05	0.64	0.56	0.28
Tm	1	0.99	0.98	0.86	0.86	0.96	-0.57	0.61	0.46	0.17	0.17	0.19	-0.05	0.18	0.53	0.51	0.11
Yb	1.00	1	0.98	0.80	0.79	0.93	-0.52	0.58	0.39	0.14	0.14	0.21	-0.06	0.20	0.45	0.45	0.07
Lu	0.99	1.00	1	0.81	0.80	0.92	-0.50	0.56	0.38	0.15	0.15	0.27	-0.11	0.26	0.48	0.50	0.01
REE	0.77	0.76	0.76	1	1.00	0.96	-0.77	0.78	0.79	0.29	0.29	-0.14	-0.08	-0.05	0.83	0.68	0.44
LREE	0.73	0.72	0.72	1.00	1	0.96	-0.77	0.77	0.79	0.29	0.29	-0.15	-0.08	-0.05	0.83	0.68	0.44
HREE	0.98	0.98	0.97	0.83	0.79	1	-0.73	0.75	0.67	0.23	0.23	-0.03	-0.03	0.01	0.70	0.58	0.35
SiO ₂	0.12	0.12	0.14	-0.07	-0.08	-0.03	1	-0.98	-0.87	-0.18	-0.18	0.25	-0.10	0.41	-0.81	-0.52	-0.71
Al ₂ O ₃	-0.28	-0.28	-0.30	-0.25	-0.25	-0.21	-0.65	1	0.81	0.12	0.12	-0.18	-0.06	-0.33	0.80	0.55	0.64
Fe ₂ O ₃	0.18	0.18	0.18	0.30	0.30	0.29	-0.77	0.37	1	0.42	0.42	-0.39	-0.06	-0.34	0.89	0.63	0.72
MnO	0.19	0.18	0.18	0.47	0.49	0.29	-0.48	-0.05	0.69	1	-0.22	-0.20	-0.16	0.21	0.30	0.27	0.27
MgO	0.10	0.12	0.13	0.04	0.02	0.18	-0.43	0.20	0.62	0.28	1	0.12	0.24	-0.18	0.56	0.26	0.37
Na ₂ O	-0.19	-0.21	-0.22	-0.12	-0.12	-0.14	-0.45	0.35	0.19	0.41	0.07	1	-0.08	0.83	-0.13	0.10	-0.84
CaO	-0.22	-0.20	-0.21	-0.28	-0.29	-0.15	-0.54	0.26	0.31	-0.03	0.47	0.00	1	-0.28	-0.18	-0.34	0.14
K ₂ O	0.48	0.48	0.47	0.32	0.30	0.40	0.40	-0.28	-0.29	-0.12	-0.04	-0.18	-0.28	1	-0.04	0.23	-0.87
TiO ₂	0.21	0.20	0.21	0.52	0.53	0.32	-0.60	0.20	0.83	0.75	0.37	0.12	0.04	-0.21	1	0.81	0.46
P ₂ O ₅	-0.29	-0.29	-0.30	-0.27	-0.26	-0.30	-0.06	0.22	-0.08	-0.48	-0.11	-0.39	0.22	-0.14	-0.11	1	0.13
CIA	0.37	0.37	0.40	0.52	0.52	0.42	-0.08	-0.33	0.37	0.44	0.02	-0.27	-0.23	-0.25	0.46	-0.32	1

The mean values of CIA are slightly higher in lowland than upland Vertisols. Their values ranged from 44.27 to 78.48%, with an average value of 64.80% in the upland Vertisols and 54.66 to 92.13%, with an average of 77.34% in the lowland Vertisols (Table 4), reflecting their higher clay mineral contents. Differences in weathering degrees of Vertisols developed on upland and lowland in the same climatic conditions are reflections of their content fraction and mineralogical differences in soils. The high quantities of resistant minerals (e.g. muscovite and quartz, Table 3) and low content of clay minerals (e.g. smectite and kaolinite, Table 3) in the upland Vertisols for instance, cause low values of CIA (Table 4). The mean CIA values in the Vertisols were globally slightly lower than CIA in the Lixisols (68.51%) and Ferralsols (79.35%) and Andosols (81.83%) (Table 4). These results demonstrate that the mineralogy of these soils has not yet exhibited complete kaolinitisation and maintains a significant quantity of mobile elements [53].

4.3.2. Trace Element Distribution in Vertisols

Trace elements have higher average values in lowland Vertisols, including Ba (851.54 ppm), Cr (513.33 ppm), Zr (496.48 ppm), Sr (165.95 ppm) and Rb (101.09 ppm) than in upland Vertisols with chromium (524.95 ppm), Ba (506.99 ppm), Sr (453.87 ppm) and Zr (295.80 ppm) (Table 4). Some elements such as chromium have highest concentration in the upland Vertisols meanwhile barium has the highest in the lowland Vertisols. Element with moderate contents are rubidium, V, Zn, Ni, Y, Cu, Ga, Co, W, Pb, Th, Hf and Nb but the other element usually have very low contents less than 3 ppm.

4.3.3. REE Distribution Patterns in Vertisols

The mean concentration of REEs in this study were summarized and shown in Table 4. A summary of the main statistical parameters (mean, maximum, minimum, and SD) was added as well. These values are higher in lowland than upland Vertisols. The concentration of REEs ranged from 148.24 to 463.75 ppm, with an average value of 275.64 ppm and 24.70 to 313.25 ppm, with an average of 137.50 ppm, respectively. Thus, the mean REE contents in the Vertisols were slightly higher than the measured mean concentrations of REE in the Lixisols (90.71 ppm) and Ferralsols (99.22 ppm) and lower than Andosols (1167.94 ppm) (Table 4, Figure 5). The highest REE contents are found in a soils order: Andosols > Lowland Vertisols > Upland Vertisols > Ferralsols > Lixisols. The elevated REE concentration in the Andosols samples can be explained by the contribution of basic rocks and the presence of halloysite to soil formation. [27], also observed that a large REE variation is highly dependent on soil type and parent materials. Thus, the soils issued from basic rocks frequently exhibit REE enrichment. Meanwhile, REE enrichment in Vertisols can be explained by high content of clay minerals (smectite and kaolinite). In general, REE concentrations increase with decreasing particle size; hence, clayey soils

exhibit higher REE concentrations than sandy soils [1]. Laveuf and Cornu [31] have demonstrated that the fractionation of REEs by clay minerals thus depend on the clay composition of the soils. Thus, chlorite shows the highest REE contents. Smectite and montmorillonite are depleted, while chlorite is enriched in REEs compared to LREEs and HREEs. Smectite and kaolinite are enriched in HREEs compared to LREEs, while illite and vermiculites are enriched in LREEs.

The concentrations of LREE and HREE follow the same behavior as those of REE. Their average LREE values ranged from 254.03 and 123.71 ppm, and those of HREE from 21.61 and 13.79 ppm, respectively. LREE represents 92% of the mean REE concentrations in Vertisols indicating that LREE are more abundant in soils than HREE. It is generally agreed that LREE are less mobile than HREE, and there is a consequent enrichment in LREE relative to HREE in the soil samples. According to Silva et al. [54] LREE enrichment and HREE depletion in soils is a consequence of the weathering processes.

Vertisols developed an upland and lowland under tropical seasonally contrasted climate showed the following orders for REE concentrations: Ce > Nd > La > Pr > Sm > Gd > Dy > Yb > Er > Eu > Ho > Tb > Lu > Tm and Ce > La > Nd > Pr > Sm > Gd > Dy > Yb > Er > Eu > Ho > Tb > Lu > Tm, respectively. Cerium, La and Nd presented enrichment in the Vertisols, and Ce presented the most abundant among the REEs with an average concentration of 120.14 ppm and 52.01 ppm, respectively for lowland and upland Vertisols. Similar results were obtained by Chittamart [9] in Thailand Vertisols and were indicated that high Ce concentrations may result from the fact that Ce can occur in a Ce (IV) valence state and may preferentially accumulate in soil.

Concentration and characteristic parameters of REEs, including $(La/Yb)_N$, $(La/Sm)_N$, $(Gd/Yb)_N$, Ce/Ce^* and Eu/Eu^* , were calculated and shown in Table 4. These parameters indicated significant fractionation of rare earth elements in soils. $(La/Yb)_N$ reflects the fractionation between REEs, $(La/Sm)_N$ between LREEs and $(Gd/Yb)_N$ reflects the fractionation between HREEs. These values are slightly higher in lowland than upland Vertisols (Table 4). The $(La/Yb)_N$ values in the upland Vertisols ranged from 4.46 to 13.69 with an average value of 8.78. They varied from 7.38 to 17.13 with an average value of 13.04 in Lowland Vertisols, indicating that the curve was right oblique and LREE-enriched. The values of $(La/Sm)_N$ ranged from 2.12 to 3.93 and 3.46 to 4.53, with an average value of 3.13 and 4.08, indicating that LREEs had significant fractionation, respectively in upland and lowland Vertisols. The values of $(Gd/Yb)_N$ ranged from 1.14 to 2.33, with an average value of 1.72 in the upland Vertisols and 1.37 to 2.24, with an average of 1.86 in the lowland Vertisols (Table 4). This indicated that HREE had no significant fractionation.

The values of Ce/Ce^* and Eu/Eu^* were calculated to determine the nature of the anomalies in Ce and Eu (Table 4 and Figure 6a and b). Rare earth pattern of the upland Vertisols

normalized to chondrite, show the same evolution in the profiles, which suggests that the materials derive from the same source and confirms their differentiation insitu from the parent rocks. Cao *et al.* [8] have demonstrated that when the Ce/Ce^* and Eu/Eu^* in soils surface values were > 1.05 , there was positive anomalies. When the Ce/Ce^* and Eu/Eu^* values were < 0.95 , there was negative anomalies. The Ce/Ce^* values ranged from 0.62 to 1.36, with an average value of 1.07 and 0.17 to 1.22, with average value 1.05 in upland and lowland, respectively, demonstrating significant positive Ce anomaly in the Vertisols. However, the values of Eu/Eu^* ranged from 0.36 to 1.87, with an average value of 0.88 in upland (Figure 6a) and 0.59 to 0.75, with an average value of 0.88 in lowland (Figure 6b), demonstrating significant negative Eu anomaly in the Vertisols. The variation in Ce anomalies in the Vertisols

can be explained by the variability of the oxidation conditions [38]. The positive Ce anomalies are linked to the oxidation of Ce^{3+} to Ce^{4+} which is stable in weathering profile [31]. The low fractionation degree of REE may be due to the environment which is not well drained and the homogenization of the profiles by seasonal deep surficial desiccation cracks.

The high LREE/HREE (8.97 and 11.75) and negative Eu anomalies (0.88 and 0.71) (Table 3) in the upland and lowland Vertisols indicates, overall, upper crustal felsic sources, which are dominant in the drainage in this zone. This result indicated that the REEs accumulated in the Vertisols may be related to natural sources (parent materials). The climate in northern Cameroon is warm and moist, and the biological effect and chemical weathering were relatively strong.

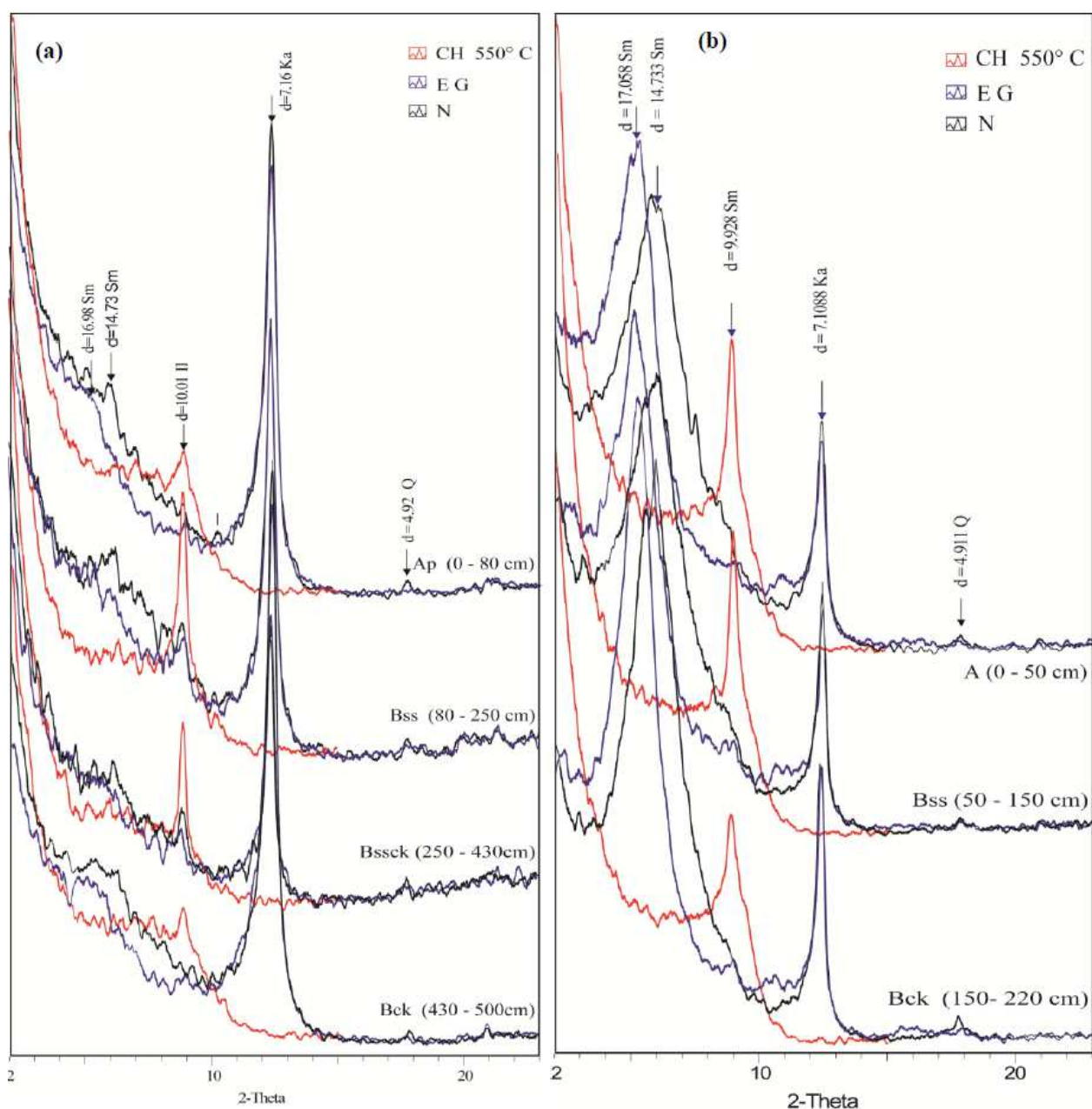


Figure 3. DRX powder patterns of the soil: (a) Lowland Vertisols and (b) Upland Vertisols.

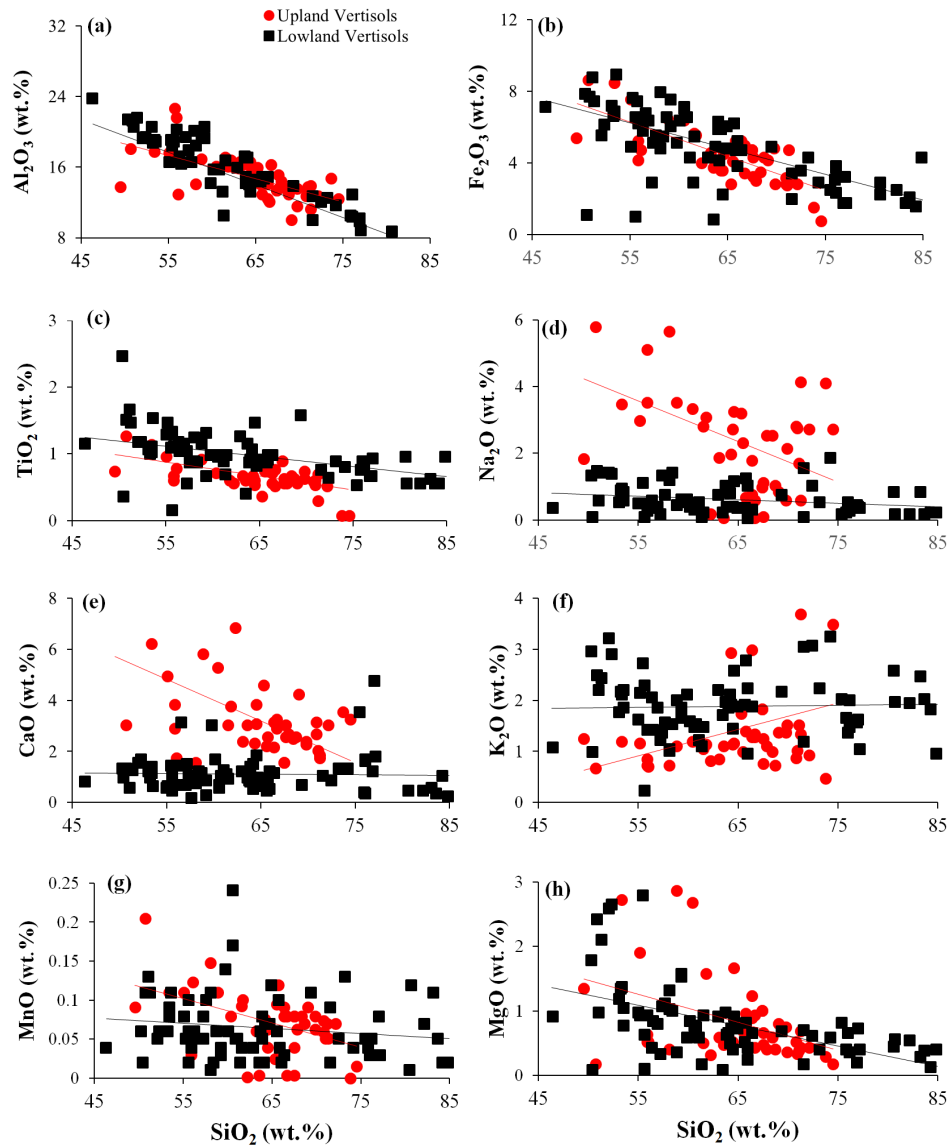


Figure 4. Harker diagrams of major elements in upland and lowland Vertisols of Northern Cameroon: (a) SiO_2 vs. Al_2O_3 ; (b) SiO_2 vs. Fe_2O_3 ; (c) SiO_2 vs. TiO_2 ; (d) SiO_2 vs. Na_2O ; (e) SiO_2 vs. CaO ; (f) SiO_2 vs. K_2O ; (g) SiO_2 vs. MgO and (h) SiO_2 vs. MnO .

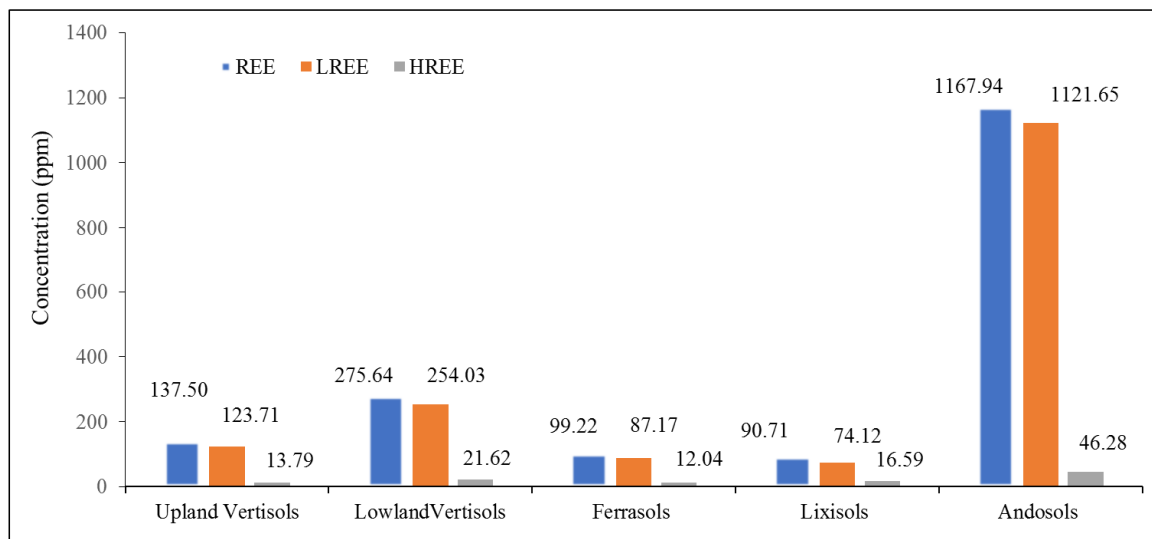


Figure 5. Graf of mean REE concentration in Vertisols compared to Ferrasols, Lixisols and Andosols data.

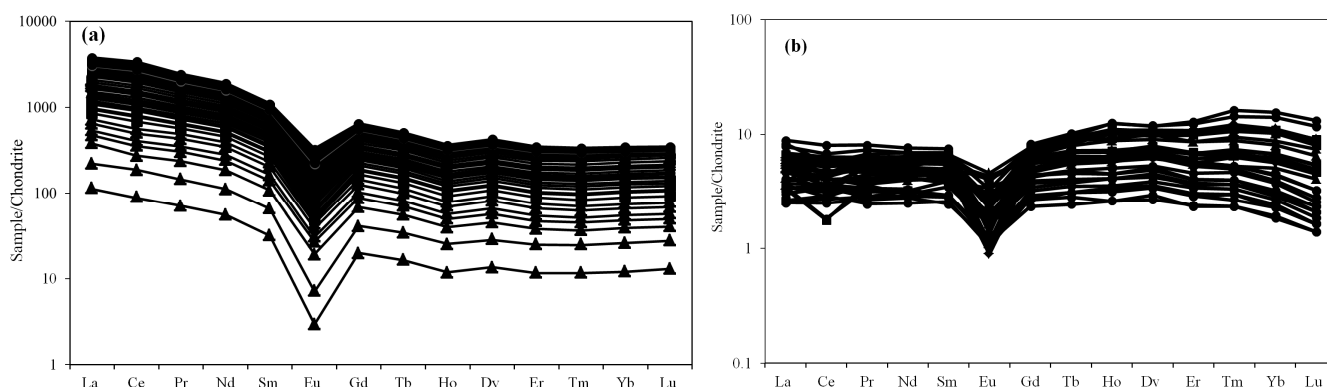


Figure 6. REE patterns normalized to chondrite values (with [50]): (a) Lowland Vertisols and (b) Upland Vertisols.

4.4. Controls on Chemical Composition of Vertisols

Factor analysis of standardized raw data for major, trace and rare earth element concentrations, and other important properties (sand, silt and clay contents, CEC, pH, OM, CEC, Smc, Sm-Kao, Kao, Il, Fe, and Q) were used to identify affinity groups globally of Vertisols parameters. The first two factors explain only 63.74% of the variation in the data (Figure 7a, b). The grouping of properties into affinity groups is mostly weak with properties showing a diffuse distribution with no very distinct affinity groups. Factor 1 describes 53.23% of the variation and significant positively covaries with% Clay, Smc, CEC, Al_2O_3 , Fe_2O_3 , TiO_2 , MnO, CIA, V, Co, Ga, Zn, Ni, Cu, Co and REE (Figure 7a) shows that clay minerals are essential in controlling REE contents in these Vertisols. We also observe negatively covaries with% Sand, %OM, pH, SiO_2 , CaO, $\text{Na}_2\text{OP}_2\text{O}_5$, Fe, Q, W, Mo, Cr and Sr. This result shows that, the total REE contents in soils are closely related to the percentage of clay, and silt-sized particles and REE are generally enriched in clay and silt fractions, but depleted in sand fraction, because of dilution by quartz and feldspar [1]. The significant positive correlations between Fe_2O_3 , MnO and REE (Figure 7a) indicate that, besides the clay minerals, the Fe–Mn–oxy–hydroxides are also controlling the total REE contents in the Vertisols. Chittamart *et al.* [9] found similar correlations between REE and Fe and Mn in the Vertisols under tropical savannah climate in Thailand. Fe–Mn–oxy–hydroxides are enriched in the fine fraction of the Vertisols and have a strong adsorptive capacity for REEs [51].

Concentrations of most trace elements (V, Co, Ga, Zn, Ni and Cu) show significant positive correlations where V and Cu show high correlation with Al showing their retention in clays, Zn and Co show high correlation with Fe, and Ga, Ni show high correlation with Ti (Figure 7a). Aluminum, Fe, Co, V and Cu are closely associated because they occur in clay mineral and oxide structures [53]. Gallium and Ni are also closely associated as they occur in titanium oxides [51]. Zr and Hf display a similar behaviour suggesting their incorporation in the same phases such as zircon [39].

Factor 2 only describes an additional 11.91% of the variation. Two affinity groups were also recognized, the first group is positively correlation with% Sand, CaO, Na_2O , MgO,

Sr and rare earth elements, and negatively covaries with% Clay, CEC, Al_2O_3 , Fe_2O_3 , TiO_2 and MgO.

Figure 7b shows the distribution biplot of soil samples and associates them in three distinct groups. The first group contains soils with high values in clay and associated properties. There are Bss horizon which enrichment in smectite and made up of lowland Vertisols. The second group has high silt content. The third group contains horizon with high values of sand as Bck horizon slightly weathering material. They consist essentially of the horizon of depth of the upland Vertisols.

Statistical analysis was used to investigate the controls on chemical composition of Vertisols and Pearson's correlations between the geochemical associated with Vertisols properties were shown in Table 5. We notice that, the correlation analysis between REEs in Vertisols samples showed (1) highly significant correlations between elements of the LREE group and (2) highly significant correlations between HREEs. REE has significant positive correlations ($r \geq 0.80$) with Al_2O_3 , Fe_2O_3 , TiO_2 , and P_2O_5 in the upland and lowland Vertisols and significant negative correlations ($r \leq -0.8$) with SiO_2 in lowland Vertisols. The high correlation of TiO_2 with LREEs ($r = 0.83$), HREEs ($r = 0.70$), and Fe_2O_3 ($r = 0.9$) (Table 5) suggests that these refractory minerals together with secondary phosphate minerals control the distribution of REEs in Vertisols.

Factor plots (Figure 8) show the element and sample affinity groups for lowland and upland Vertisols. By separately considering affinity groups of elements for lowland and upland Vertisols, the first two factors for lowland soils explain 60.16% of variation (Figure 9a) whereas for upland Vertisols the first two factors explain only 50.03% (Figure 9b). The high value in lowland Vertisols can be explained by the homogeneity of the materials along the profiles and indicated that the composition of soils is quite uniform within the profile and that differentiated sedimentary layering has not been preserved or that pedoaccumulation of clay. Furthermore, lower value of upland Vertisols explains the absence of the affinities of the elements in the group. Similar results have been obtained by Chittamart *et al.* [9] who indicates that the absence of distinct affinity groups of elements for upland Vertisols may reflect the relative immaturity of these soil profiles which contain relatively large amounts of residual primary minerals.

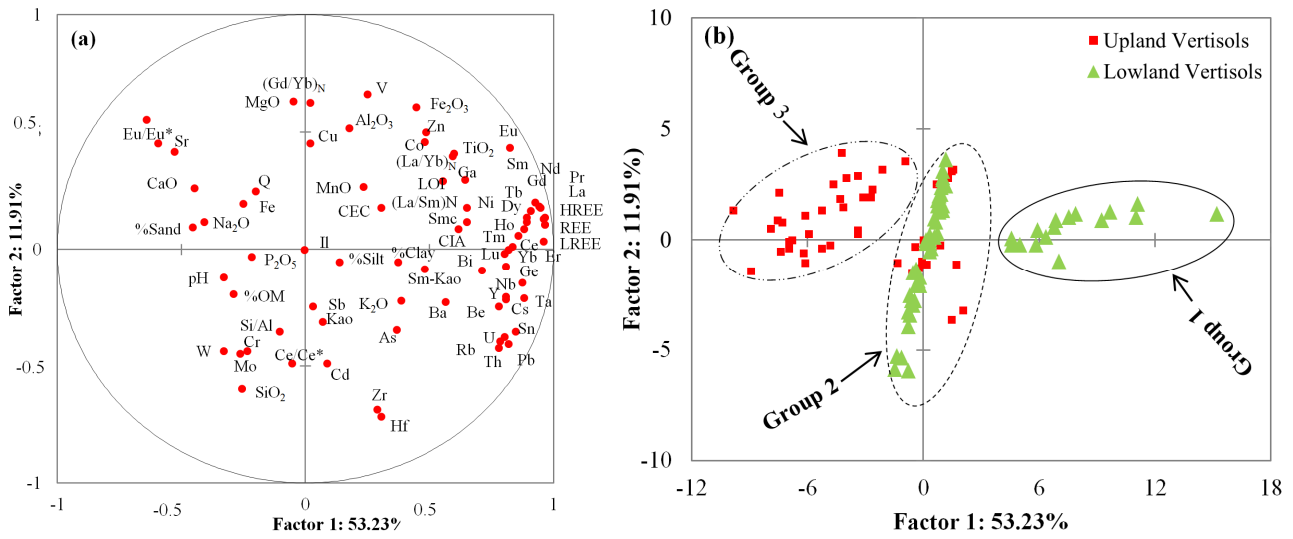


Figure 7. Factor analysis based on chemical properties of bulk soil samples of Vertisols (a) distribution of chemical properties (variables) and (b) distribution of soils samples (cases).

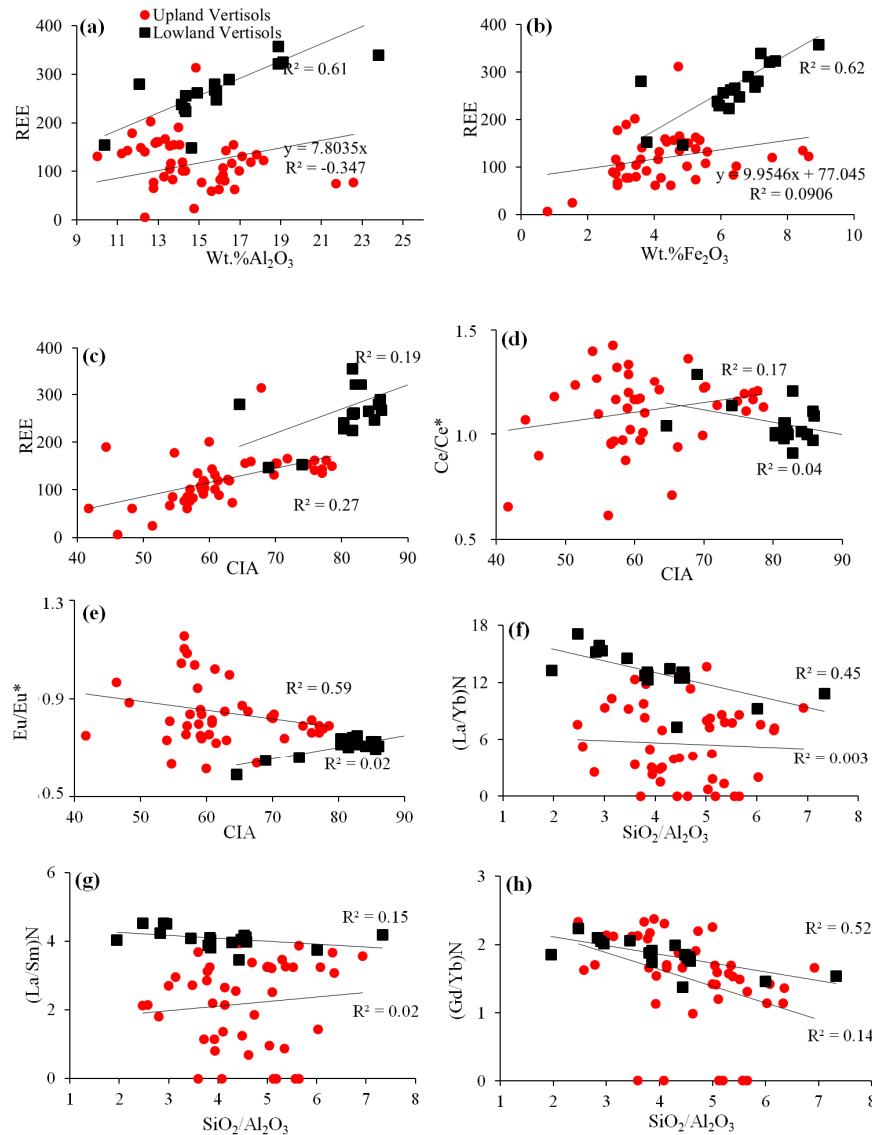


Figure 8. Factor plots showing the element and sample affinity groups for lowland (a) and upland (b) Vertisols.

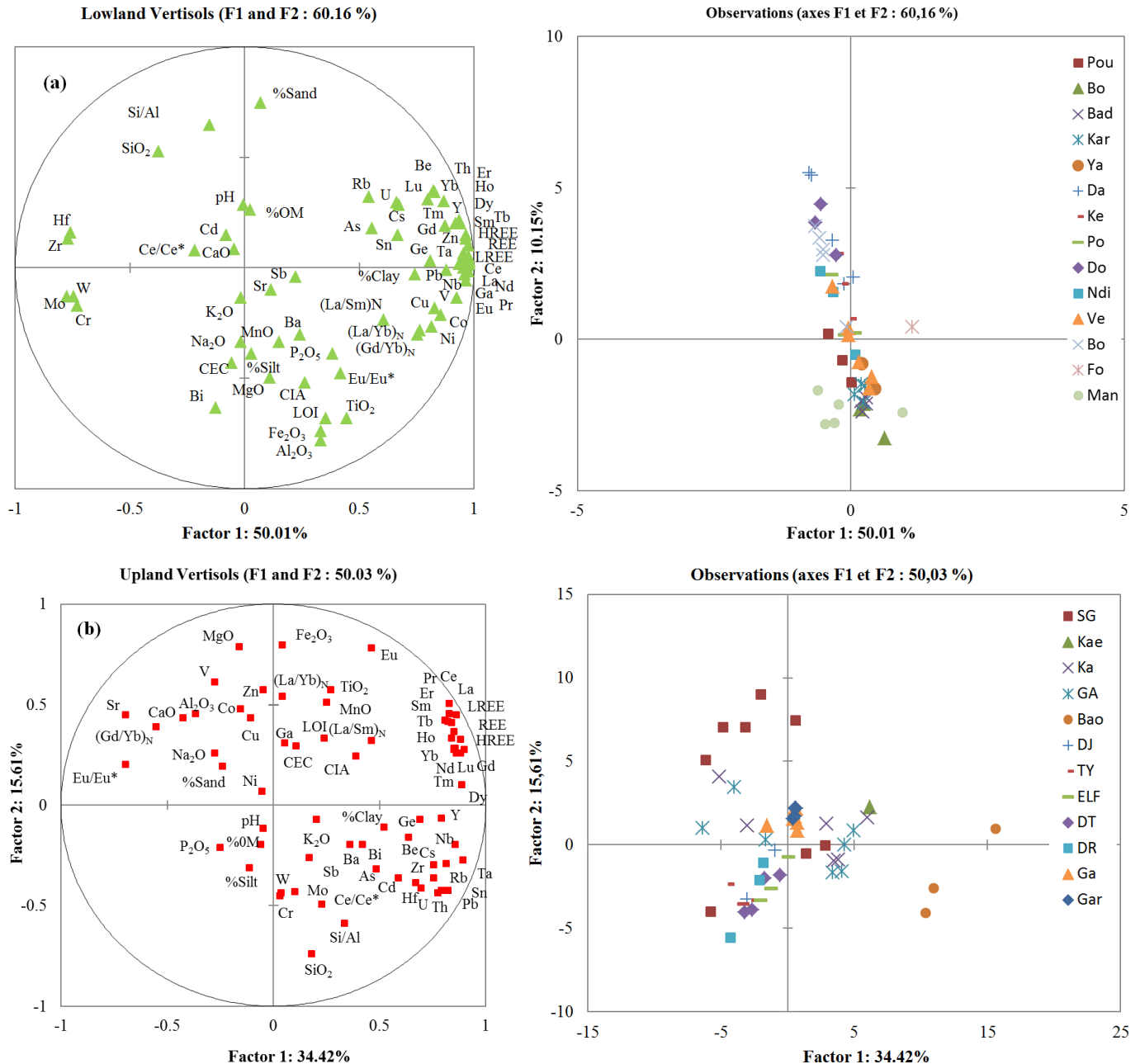


Figure 9. Factor plots showing the element and sample affinity groups for lowland (a) and upland (b) Vertisols.

4.5. Genesis of Smectites in Vertisols

Smectites formation requires some environmental conditions such as flat zones, poor drainage and contrasting dry and wet seasons [15, 48, 49, 30]. All these conditions are fulfilled in the studied zone. The use of particle size data made it possible to follow the genesis in upland and lowland Vertisols. In the upland Vertisols, genesis of the smectites is made from the feldspars present in the parent rock (granite, metadolerite and gneiss) [42, 48]. In fact, the alteration of the feldspars leads to the exclusive neoformation of a relatively well crystallized smectite. It is carried out in "glove fingers" on plagioclase feldspar and is massive on potassium feldspar. In both cases, the alteration is centripetal. Geochemically, it

translates into partial leaching of silica and potassium and a relative concentration of Al_2O_3 , Ca, Na, and Mg, all of which are involved in the formation of smectite [48, 30]. In addition, it also results in partial leaching of cerium and europium. Kawano and Tomita [28] showed experimentally that smectite formation by alteration of feldspar occurs in three steps: (1) formation of a thin leached layer on the feldspar surface; (2) non-crystalline fibres grow within the leached layer; and (3) smectites are formed from the fibrous phases.

In lowland Vertisols, the high smectite content was related to the low landscape positions, a strongly contrasted climate and the presence of a clay-rich alluvial parent material [9, 59]. The simultaneous occurrence of kaolinite in the profiles could be related to light and successive variations in drainage conditions. The combination of those factors enhanced the

relative concentration of alkaline and alkali-earth cations alongside silica favorable to the neoformation and conservation of smectite [14, 48]. Recent researches have explained their formation with the presence of soil modifiers such as Ca-zeolites that release Ca^{2+} ions to prevent the complete transformation of smectite to kaolin, and the high base status helps in stabilizing and retention of smectite [48, 29]. The landscape position of the studied Vertisols might have boosted smectite synthesis by heritage from downslope accumulation of some rock-forming silicates and neoformation [23, 43]. The major smectites component of these soils influences their physic and chemical properties; and is responsible of the formation of specific features described above: crack desiccation, gilgai and slickensides. In the lowland Vertisols, there are two major sources of clay minerals: i) the most common silicate clay minerals are those inherited from the parent material, and ii) minerals arising from pedogenesis [36].

4.6. Vertisolization Process

The climate of northern Cameroon has characteristics favourable to vertisolization. The climatic and soil water balance study showed that after a long period of waterlogging (6 months) at cool temperatures (average temperature of the coldest month 12 to 15°C), it observe periods of progressive drying (2 months) at hot temperatures (average temperature of the hottest month 30 to 35°C). The upland Vertisols will undergo these alternations of waterlogging and drying: during the hydromorphic period, the cool temperatures are partly responsible for an inactive microbial life, and for a slow decomposition of the organic matter which can accumulate by default destruction.

In the case of lowland Vertisols, the drying period can be reduced since the lowland areas receive runoff from the surrounding landscape [9]. The drying periods are therefore much shorter than in the case of upland Vertisols. During the warm period, the soil remains moist due to a supply of water from severe thunderstorms and the subsequent runoff; microbial life is intense and organic matter not protected by clay is destroyed. In addition, this soil moisture during the hot period slows down the polymerization of gray humic acids, which requires sufficiently long periods of drying.

The neoformation of smectites which requires a medium rich in alkaline and alkaline-earth cations and especially poor drainage, such that the rate of hydrolysis of minerals is greater than that of evacuation of the ions in solution, finds a favourable environment for its training. The most soluble ions (Ca, Na, K) can be removed, the others (Al, Si, Mg, Fe) will reorganize into smectites [48, 30]. The high topographic position of the upland Vertisols does not allow a replenishment of Ca^{2+} and Mg^{2+} ions, other than that resulting from the alteration of the alterable primary minerals present in the horizon (feldspar and mica). On the other hand, in the lowland Vertisols the resupply of cations of the surface horizons can be achieved by runoff from upstream.

The abundant rainfall in the cool and wet season can be

used to explain cation leaching, the slight desaturation of the surface horizon complex and the relatively acidic pH. The high topographic position does not allow a replenishment of Ca^{2+} and Mg^{2+} ions, other than that coming from the alteration of the alterable primary minerals present in the horizon (plagioclases, augite) [14, 30, 48]. On the other hand, in the lowland Vertisols the resupply of cations to the surface horizons can be achieved by runoff from upstream. In upland Vertisols, another form of replenishment of the surface horizons can be mentioned: "piezoturbation" rises to the surface of the material of the lower horizons. In the Vertisols of northern Cameroon, this rise in elements is very weak and slow as shown by microscopic studies, insufficient in any case to balance the losses. The importance of pedoturbation depends largely on the slow or fast alternation of the drying moisture cycles. The relatively humid climate of northern Cameroon, without brutally contrasting seasons, limits the possibilities of soil drying and therefore slows down the mechanical "turn-over" of the elements. These reflections join that of De Carloa and Caylor [13], who experimentally has shown that the amplitude of the swelling is a function of drying (i) the more smectite type clay dries up and the more it swells, and (ii) in this case the piezoturbation is exacerbated. In lowland Vertisols, the pedoturbation is even lower, but the replenishment is ensured thanks to the topographic position.

5. Conclusion

The objective of the present work was to determine the geochemical of the Vertisols on lowland and upland areas under tropical seasonally contrasted climate in Northern Cameroon. Macro-micromorphological, physico-chemical, mineralogical and geochemical properties were investigated to assess the genesis of smectite and vertisolization processes on their geochemistry relation. The following conclusion can be drawn from this work:

1. Vertisols are deep, dark grey, heavy clayey, massive, compact and very dense ($1.7\text{--}2.2 \text{ g/cm}^3$); it show high cation exchange capacity, high sum of exchangeable bases, high base saturation, low to high organic matter, low to high available phosphorus and low total nitrogen; and the most abundant mineral is smectite, but small amounts of kaolinite and illite, and traces quartz, feldspars are present.
2. Chemical composition is dominated by silicon (50.35-59.42% SiO_2), aluminium (16.52-21.61% Al_2O_3) and iron (4.86-7.96% Fe_2O_3), but basic cations are also homogeneously concentrated in the profiles. Low topographic position, a strongly contrasted tropical climate with a long dry season and a clay-rich alluvial material has favoured smectite synthesis.
3. Vertisols developed upland and lowland under tropical seasonally contrasted climate showed the following orders for REE concentrations: $\text{Ce} > \text{Nd} > \text{La} > \text{Pr} > \text{Sm} > \text{Gd} > \text{Dy} > \text{Yb} > \text{Er} > \text{Eu} > \text{Ho} > \text{Tb} > \text{Lu} > \text{Tm}$ and $\text{Ce} > \text{La} > \text{Nd} > \text{Pr} > \text{Sm} > \text{Gd} > \text{Dy} > \text{Yb} > \text{Er} > \text{Eu} > \text{Ho} > \text{Tb} > \text{Lu} > \text{Tm}$, respectively.

4. Genesis of the smectites is made from the feldspars present in the parent rock in the upland Vertisols; meanwhile, high smectite content was related to the low landscape positions, a strongly contrasted climate and the presence of a clay-rich alluvial parent material in lowland Vertisols.
5. Climates with contrasting seasons, there is intense weathering during the wet season. The released ions are concentrated in the dry season and give smectite. This concentration can take place on site on basic or acid crystal rocks, or in the low points of the landscape.

Acknowledgements

The authors declare that they have no competing financial, knowledge, personal interests or relationships that could have influenced the work reported in this article.

References

- [1] Alfaro, M. R., do Nascimento, C. W. A., Biondi, C. M., et al., 2018. Rare-earth-element geochemistry in soils developed in different geological settings of Cuba. *Catena*, 162, 317-324.
- [2] Aydinalp, C., 2010. Some important properties and classification of vertisols under Mediterranean climate. *Afr. J. of Agricultural Research*, 6, 449-452.
- [3] Azinwi, P. T., Djoufack-Woumfo, E., Bitom, D., Njopwouo, D., 2011. Petrological, physico-chemical and mechanical characterization of topomorphic vertisols from the sudanohelien region of North Cameroon. *Bentham Open Geology Journal* 5, 33-55.
- [4] Banakeng, L. A., Zo'o Zame, P., Tchameni, R., Mamdem, L., Bitom, D., 2016. Mineralogy and geochemistry of laterites developed on chlorite schists in Tchollire region, North Cameroon. *Journal of African Earth Sciences*, 119, 264-278.
- [5] Barrault, J., Eckebil, J. P., Vaille J., 1972. The work of IRAT on transplanted sorghum in North Cameroon. *Trop. Agronomist*, 27, 791-814.
- [6] Brabant, P., Gavaud M., 1985. Les sols et les ressources en terres du Nord Cameroun (Province du Nord et de l'Extrême-Nord ORSTOM-MESRES-IRA, Paris, 285p.
- [7] Bremner, J. M., Mulvaney, C. S., 1982. Total Nitrogen, in *Methods of Soil Analysis, Part 2, Chemical Analysis*, D. R. Buxton, Ed. Madison: American Society of Agronomy Inc. and Soil Science Society of America Inc., 595-624.
- [8] Cao, X., Chen, Y., Wang, X., Deng, X., 2001. Effects of redox potential and pH value on the release of rare earth elements from soil. *Chemosphere*, 44 (4), 655-661.
- [9] Chittamart, N., Suddhiprakarn, A., Kheoruenromne, I., Gilkes, R. J., 2010. The pedo-geochemistry of Vertisols under tropical savanna climate. *Geoderma*, 159, 304-316.
- [10] Cook, H. E., Johnson, P. D., Matti, J. C., Zemmels, I., 1975. Methods of sample preparation and X-ray diffraction data analysis in X-ray mineralogy laboratory: in *Initial Reports of the DSDP* (A. G. Kaneps, editor). Printing Office, Washington, D.C., 997-1007.
- [11] Coulombe, C. E., Wilding, L. P., Dixon J. B., 1996. Overview of Vertisols: characteristics *and* impacts on society. *Advances in Agnomomy*, 57, 289-375.
- [12] Coulombe, C. E., Dixon, J. B., Wilding, L. P., 2006. Mineralogy and physical chemistry of vertisols. In: *Vertisols and technology for their management*, M. Ahmad and A. Mermut (Eds.), Texas A and M University, Texas, Elsevier Science Publishers, 115-200.
- [13] DeCarlo, K. F., Caylor, K. K., 2019. Biophysical effects on soil crack morphology in a faunally active dry land vertisol, *Geoderma*, 334, 134-145.
- [14] Djordjevic, A., Golubovic, S., Zorica, T., Velimir, A., Natasa, N., Olivera, J., 2012. The origin of montmorillonite in vertisols from the Southern Serbian Peinja District. *African Journal of Agricultural Research*, 7, 20, 3034-3044.
- [15] Duchaufour, P., 1977. *Pédogenèse et classification des sols*. Masson (Eds.), Paris, 492p.
- [16] Dudal, R., Eswaran H., 1988. Distribution, properties and classification of vertisols. In: *Vertisols: their distribution, properties, classification, and management*. Wilding L. P. and Puentes R. (Eds.), Technical Monograph No. 18, Texas A and M University Printing Center, College Station, Texas, 1-22.
- [17] Esu, I. E., Lombin, G., 1988. Characteristics and management problems of vertisols in the Nigerian Savannah. In: *proceedings of a Conference held at ILCA on the Management of Vertisols in Sub-Saharan Africa*. S. C. Jutsi, I. Haque, J. McIntire and J. shares, Eds., Adis Ababa, Ethiopia, 293-307.
- [18] Eswaran, H., Cook, T., 1988. Classification and management related properties of vertisols. In: *proceedings of the of a Conference held at ILCA on the management of vertisols in Sub-Saharan Africa*, S. C. Jutsi, I. Haque, J. McIntire and J. shares (Eds.), Adis Ababa, Ethiopia, 64-84.
- [19] Etame, J., Gerard, M., Bilong, P., Suh, C. E., 2009. Behaviour of elements in soils developed from nephelinites at Mount Etinde (Cameroon): Impact of hydrothermal versus weathering processes. *J. Afr. Earth Sci.*, 54, 37-45.
- [20] FAO, 2006. Guidelines for soil description, a framework for international classification, correlation and communication. *FAO-ISRIC-IUSS*, 4th edition, Rome, 128p.
- [21] Fassil Kebede 2009. Silicon status and its relationship with major physico-chemical properties of vertisols in of Northern Highlands of Ethiopia. *College of Dryland Agriculture and Natural Resource Management journal*, 1, 74-81.
- [22] Fitzpatrick, E. A., 1984. *Micromorphology of soils*. Chapman and Hall, New York, 433p.
- [23] Gala'n, E., 2006. Genesis of clay minerals. In: *Handbook of Clay Science*, F. Bergaya, B. K. G. Theng, G., Lagaly (Eds.), *Developments in Clay Science* 1, Elsevier, 1129-1162.
- [24] Gavaud, M., Rieffel, J. M., Muller, J. P., 1975. Les sols de la vallée de la Bénoué, de Lagdo jusqu'au confluent du Faro. *ORSTOM, Bondy*, 690p.
- [25] Hallsworth, E. G., Robertson, E. G., Gibbon, F. R., 1955. *Studies in pedogenesis in New South Wales 8: The gilgai soils*. *Soil Sci.*, 6, 1-31.
- [26] Hammad, M. A. M., Abou EL-Enan, S. M., EL-Ashry, Kh., Samy A., 2017. Micromorphological Studies of some Egyptian Soils. *J. Soil Sci. and Agric. Eng., Mansoura Univ.*, 8 (9), 391-394.

- [27] Hu, Z., Haneklaus, S., Sparovek, G., Schnug, E., 2006. Rare earth elements in soils. *Commun. Soil Sci. Plant Anal.*, 37, 1381-1420.
- [28] Kawano, M., Tomita, K., 1992. Formation of allophane and beidellite during hydrothermal alteration of volcanic glass below 200°C. *Clays and Clay Minerals*, 40, 666-674.
- [29] Kovda, I., Goryachkin, S., Lebedeva, M., Chizhikova, N., Kulikov, A., Badmaev, N., 2017. Vertic soils and Vertisols in cryogenic environments of southern Siberia, Russia. *Geoderma*, 288, 184-195.
- [30] Kovda, I., 2020. Vertisols: extreme features and extreme environment. *Geoderma Regional*, 22, <https://doi.org/10.1016/j.geodrs.2020.e00312>.
- [31] Laveuf, C., Cornu, S., 2009. A review on the potentiality of rare earth elements to trace pedogenetic processes. *Geoderma* 154, 1-12.
- [32] Lim, C. H., Jackson, M. L., 1986. Expandable phyllosilicate reactions with lithium on heating. *Clays and Clay Minerals*, 34, 346-352.
- [33] Mamo, T., Haque, I., 1988. Potassium status of some Ethiopian soils. *East African Agricultural and Forestry Journal*, 53, 123-130.
- [34] McLean, E. O., 1982. Soil pH and lime requirement, in *Methods of Soil Analysis, Part 2, Chemical and Microbiological Properties*, D. R. Buxton, Ed. Madison: American Society of Agronomy Inc. and Soil Science Society of America Inc., 199-224.
- [35] Moore, D. M., Reynolds, R. C. 1989. X-ray Diffraction and the Identification and Analysis of Clay Minerals, 179-201.
- [36] Moustakas, N. K., 2012. A study of Vertisols genesis in North Eastern Greece. *Catena*, 92, 208-215.
- [37] Munsell Color, 2000. *Munsell Soil Color Charts, 2000 Revised Washable Edition*. Gretagmacbeth, New Windsor, NY.
- [38] Ndjigui, P.-D., Bilong, P., Bitom, D., Dia, A., 2008. Mobilization and redistribution of major and trace elements in two weathering profiles developed on serpentinites in the Lomie ultramafic complex, South-East Cameroon. *J. Afr. Earth Sci.*, 50, 305-328.
- [39] Ngo Bidjeck B. L. M., Ipan A. S., Ngena Tetsa R. K., Binam Mandeng E. P., Bitom L. D., 2019. Major and trace elements behaviour in two weathering profiles developed on gabbroic rocks in Meka'a and Abiete (south Cameroon, central Africa). *J. Afr. Earth Sci.*, 151, 241-254.
- [40] Nelson, D. W., Sommers L. E., 1982. Total Carbon, Organic Carbon and Organic Matter, In *Methods of Soil Analysis, Part 2, Chemical Analysis*, D. R. Buxton, Ed. Madison: American Society of Agronomy Inc. and Soil Science Society of America Inc., 539-579.
- [41] Nesbitt, H. W., Young, G. M., 1982. Early Proterozoic climates and plate motions inferred from majors element chemistry of laterites. *Nature*, 299, 715-717.
- [42] Nguetnkam, J. P., Kamga, R., Villie, F., Ras, Ekodeck, G. E., Yvon, J., 2007. Pedogenic formation of smectites in a Vertisols developed from granitic rock from Kaele (Cameroon, Central Africa). *Clay Minerals*, 42, 487-501.
- [43] Nguetnkam, J. P., Kamga, R., Villiéras Ekodeck, G. E., Yvon J., 2007. Weathering response of granite in tropical zone. Example of two sequences studied in Cameroon (Central Africa). *Etude et Gestion des Sols*, 14, 1, 13-41.
- [44] Nguetnkam, J. P., Kamga, R., Villiéras, F., Ekodeck, G. E., Yvon, J., 2008. Assessing the bleaching capacity of some Cameroonian clays on vegetable oil. *Applied Clay Science*, 39, 3 - 4, 113-121.
- [45] Obale-Ebanga, F., Sevink, J., de Groot, W., Nolte, C., 2002. Myths of slash and burn on physical degradation of savannah soils: impacts on vertisols in North Cameroon. *Soil Use and Management*, 19, 83-86.
- [46] Och, L. M., Müller, M., Wichser, A., Ulrich A., Vologina, E. G., Sturm, M., 2014. Rare earth elements in the sediments of Lake Baikal. *Chemical Geology*, 376, 61-75.
- [47] Olsen, S. R., Sommers, L. E., 1982. Phosphorus, in *Methods of Soil Analysis, Part 2, Chemical and Microbiological Properties* 2, A. L. Page, R. H. Buxton, D. R. Miller Keeney, Eds. Madison: American society of Agronomy, 403-430.
- [48] Pal, D. K., 2017. *A Treatise of Indian and Tropical Soils*. Nagpur, Maharashtra India, 180p.
- [49] Pal, D. K., Wani, S. P., Sahrawat, K. L., 2012. Vertisols of tropical Indian environments: Pedology and edaphology. *Geoderma*, 189-190: 28-49.
- [50] Pourmand, A., Dauphas, N., Ireland, T. J., 2012. A novel extraction chromatography and MC-ICP-MS technique for rapid analysis of REE, Sc and Y: Revising CI-chondrite and Post-Archean Australian Shale (PAAS) abundances. *Chemical Geology*, 291 38-54.
- [51] Ram, R., Becker, M., Brugger, J., et al., 2019. Characterization of a rare earth element (REE)-bearing ion-adsorption clay deposit in Madagascar, *Chemical Geology*, 522, 93-107.
- [52] Seiny-Bouker, L., Floret, C., Pontanier, R., 1992. Degradation of savana soils and reduction of water available for the vegetation: the case of northern Cameroon vertisols. *Cameroon Journal of Soil Science*, 72 (4), 459-488.
- [53] Silva, Y. J. A. B., Do Nascimento, C. W. A., Biondi, C. M., et al., 2020. Concentrations of major and trace elements in soil profiles developed over granites across a climosequence in north eastern Brazil. *Catena*, 193, 104-641, <https://doi.org/10.1016/j.catena.2020.104641>.
- [54] Silva, Y. J. A. B., Do Nascimento, C. W. A., Biondi, C. M., et al., 2017. Influence of metaluminous granite mineralogy on the rare earth element geochemistry of rocks and soils along a climosequence in Brazil. *Geoderma*, 306, 28-39.
- [55] Silva, Y. J. A. B., Nascimento, C. W. A., Van Straaten, P., Biondi, C. M., Silva, Y. J. A. B., Araújo, J. C. T., Alcantara, V. C., Silva, F. L., Silva, R. J. A. B., 2018. Rare earth element geochemistry during weathering of S-type granites from dry to humid climates of Brazil. *J. Plant Nutr. Soil Sci.* 000, 1-16.
- [56] Soil Survey Staff, 1999. *Soil taxonomy*. In: *Agriculture Handbook No. 436*, Second edition. USDA-NRCS.
- [57] Stoops, G., Marcelino, V., Mees, F., 2018. *Interpretation of Micromorphological Features of Soils and Regoliths*. 2nd ed. Elsevier Science, Amsterdam, 1000p.

- [58] Stoops, G., Langohr, R., Van Ranst, E., 2020. Micromorphology of soils and palaeosoils in Belgium. An inventory and meta-analysis. *Catena*, 194, 104-718.
- [59] Temga, J. P., Azinwi, T. P., Basga, D. S., Zo'oZame, P., Gouban, H., Abossolo, M., Nguetnkam, J. P., Bitom, D. L., 2019. Characteristics, classification and genesis of Vertisols under seasonally contrasted climate in the Lake Chad Basin, Central Africa. *J. Afr. Earth Sci.*, 150, 176-1933.
- [60] Thomas, G. W., 1982. Exchangeable cations, in *Methods of Soil Analysis, Part 2, Chemical and Microbiological Properties*, A. L. Page, R. H. Buxton, D. R. Miller Keeney, Eds., Madison: American Society of Agronomy Inc. and Soil Science Society of America Inc., 159-165.
- [61] Thorez, J., 2000. Cation-saturated swelling physicals: and XRD revisitation. in: *Proceedings of the First Latin-American Clay Conference* (C. F. Gomes, editor). Associacao Portuguesa de Argilas, Madeira. 71-85.
- [62] Yerima, B. P. K., Van Ranst, E., 2005. Major soil classification systems used in the tropics: soils.
- [63] Yerima, B. P. K., Van Ranst, E., Verdoodt A., 2009. Use of correlation relationships to enhance understanding of pedogenic processes and use potential of vertisols and verticceptisols of the Bale mountain area of Ethiopia. *Tropicultura*, 27, 4, 223-232.
- [64] Yvon, J., Lietard O., Cases J. M., 1982. Minéralogie des argiles kaoliniques des Charentes. *Bulletin de Minéralogie*, 105, 431-437.